INVESTIGATING THE DIURNAL AND WEEKLY CYCLE OF HCHO BY USING MINI MAX-DOAS OBSERVATIONS

Asadullah Shoaib

00000118833

Institute of Environmental Sciences and Engineering
School of Civil and Environmental Engineering
National University of Sciences and Technology
Islamabad, Pakistan

(2019)

INVESTIGATING THE DIURNAL AND WEEKLY CYCLE OF HCHO BY USING MINI MAX-DOAS OBSERVATIONS

A thesis submitted in partial fulfillment of the requirements for the degree of

Master of Science in Environmental Science

By

Asadullah Shoaib

00000118833

Institute of Environmental Sciences and Engineering (IESE)
School of Civil and Environmental Engineering (SCEE)
National University of Sciences and Technology (NUST)
Islamabad, Pakistan
(2019)

THESIS ACCEPTANCE CERTIFICATE

It is certified that the contents and form of the thesis entitled "Investigating the diurnal and weekly cycle of HCHO by using Mini Max-DOAS observations" submitted by **Mr. Asadullah Shoaib (Reg # 00000118833)** has been found satisfactory for the requirements of the degree of Master of Science in Environmental Science.

Supervisor: _____

Dr. M. Fahim Khokhar

IESE, SCEE, NUST

Head of Department: _____

Dr. Muhammad Arshad

IESE, SCEE, NUST

Principal: _____

Dr. Tariq Mahmood

SCEE, NUST

CERTIFICATE

It is certified that the contents and form of the thesis entitled

"INVESTIGATING THE DIURNAL AND WEEKLY CYCLE OF HCHO BY USING MINI MAX-DOAS OBSERVATIONS"

Submitted by

Asadullah Shoaib

has been found satisfactory for the requirement of the degree

Supervisor: _____
Dr. Muhammad Fahim Khokhar
Professor
IESE, SCEE, NUST

Member: _____
Dr. Muhammad Arshad
Associate Professor
IESE, SCEE, NUST

Member: _____
Dr. M. Zeeshan Ali Khan
Assistant Professor
IESE, SCEE, NUST

DEDICATION

Every challenging work needs self-efforts as well as the guidance of elders especially those who were very close to our hearts.

My humble effort I dedicate to my sweet and lovely

Father and Mother,

Whose affection, love, encouragement and prays of day and night make me able to such success and honor

ACKNOWLEDGEMENTS

All the praise and respect for **Almighty Allah**, who is the ultimate source of all knowledge and wisdom gifted to mankind.

I would like to acknowledge the friendly support and constructive criticism of my supervisor **Dr. M. Fahim Khokhar**, his never-ending guidance pushed me to complete the study successfully. I would also like to show my gratitude to GEC members, **Dr. Zeeshan Ali Khan** and **Dr. Muhammad Arshad** for their assistance.

I also want to appreciate the role of Mr. Junaid and Mr. Rizwan from IGIS for their helping attitude that allowed me to learn the application of the software used in the spatial representation of my study.

Last but not the least, many thanks also go to my Family and my C-CARGO colleagues; Junaid Khayyan Butt, Tehreem Mustansar, Zunaira Jabeen, Maryam Sarfaraz, Aimon Tanvir, Osama Sandhu, Hamad Khalid Satti, Marium Fiaz, Zara Maqsood, Rabia Akmal, Awais Javaid and HHAAT (juniors) group for being supportive for my Research.

Asadullah Shoaib

Table of Contents

LIST OF FIGURES

LIST OF TABLES

List of Abbreviations

$\mu g/m^3$	Microgram per Cubic meter
AMF	Air Mass Factor
ArcGIS	Arc Geographic Information System
C-CARGO	Climate Change and Atmospheric Research Group
DOAS	Differential Optical Absorption Spectroscopy
DOASIS	Differential Optical Absorption Spectroscopy Intelligent System
DSCD	Differential Slant Column Densities
FTIR	Fourier Transform Infrared Spectrometry
FWHM	Full Width Half Maximum
GOP	Government of Pakistan
HCHO SCD	Formaldehyde Slant Column Density
HCHO VCD	Formaldehyde Vertical Column Density
HCHO/CH2O	Formaldehyde
HNO_3	Nitric Acid
IESE	Institute of Environmental Sciences and Engineering
JICA	Japan International Cooperation Agency
LTV	Light Transport Vehicle
MAX-DOAS	Multi-axis Differential Optical Absorption Spectroscop
NGO's	Non-Government Organizations
NMVOC	Non-Methane Volatile Organic Compound
NO_2	Nitrogen Dioxide
NUST	National University of Science and Technology
O_3	Ozone
OMI	Ozone Monitoring Instrument
Pak-EPA	Pakistan Environmental Protection Agency
Pak-NEQS	Pakistan National Environmental Quality Standards

PCTs	Pollution Control Techniques
PM	Particulate Matter
ppbv	Parts per Billion by volume
RMS	Root Mean Square
SFP	Slit function Parameter
UTC	Coordinated Universal Time
UV	Ultra-Violet
VOCs	Volatile Organic Compounds
WHO	World Health Organization
WinDOAS	Windows Differential Optical Absorption Spectroscopy

Abstract

An oxygenated Volatile Organic Compound (VOC), Formaldehyde (HCHO), essentially contributes to the hazardous tropospheric ozone pollution in urban areas. Emissions from automobiles are the major contributors towards elevated formaldehyde concentrations in major urban cities of Pakistan, exposing the population to a polluted urban environment. This study was planned to quantify the formaldehyde concentration at a fixed place IESE, NUST Islamabad for a period of two years. Additionally, periodic mobile monitoring of HCHO was carried out with in cities of Lahore, Islamabad and Multan. Observations from MAX-DOAS (Multi-Axis – Differential Optical Absorption Spectroscopy) instrument was used to measure the diurnal, weekly and annual cycle in HCHO concentration at fixed site of Islamabad. The diurnal concentrations were found to increase with an increase in temperature. The weekly cycle revealed the higher values on working days and lesser values during the weekend, while the annual cycle shows the highest concentration in summer followed by spring, autumn and winter. During field campaigns the maximum mean values of HCHO over Lahore were found to be 164, 108, 283 ppb, meanwhile; the maximum mean value in Multan was 161 ppb, exceeding the limit prescribed by WHO (83 ppb). The suspected sources of HCHO at a fixed station and along routes of field campaigns were identified as natural gas consumption, biogenic emissions from vegetation, emissions from industries including brick kilns, steel mills, oil mills and vehicular emissions. Furthermore, monthly OMI satellite observations were compared with ground-based formaldehyde values. A good correlation of .68 was noticed within the time span of 6 am – 6 pm (PST).

Chapter 1

1. Introduction

1.1. Background

Atmosphere consists of a thin layer and half of its mass is present below an altitude of 5 Km. The existence of life on earth solely depends upon this thin layer, which separates the earth's surface from outer space. It provides a shield from harmful UV rays (ozone layer) by covering the entire biosphere. It also increases the surface temperature higher than freezing point (greenhouse effect), and its component are required by the living organism for their proper metabolism. Therefore, one of the most important and relevant features of science includes the understanding of the atmosphere, its processes, characteristics, and reaction to anthropogenic activity.

Anthropogenic activities affect the environment and biosphere by causing global warming (Rom et al., 2008; Ayres et al. 2009; WMO 2009) and climate change. Global temperature is increasing day by day caused by greenhouse effect mainly from anthropogenic activity. The emissions of these greenhouse are increasing day by day. The Intergovernmental Panel on Climate Change report (2007) described that the main culprit behind the detected increase in global temperature is due to rise in anthropogenic greenhouse gas emissions.

1.2. Urban Air Pollution

Transportation, energy production and industrial activity emit different types of pollutants, which cause air pollution. Due to rapid urbanization, these pollutants concentrated in densely populated areas. In megacities (10 million or more inhabitants) environmental impacts are especially adverse (e.g., Gurjar & Lelieveld, 2005). Such severe impact can be

easily noticed in some Asian countries like China and India where air quality is greatly affected by different factors, which include large population size, limitless industrial emission and vast use of the automobiles. Rapid urbanization, automobile use on large scale and unplanned industrial growth results in deteriorating the urban air quality.

1.2.1. Air Pollution

Air pollution has appeared as a potential risk for the environment and the health of living things. In megacities, the concentration of toxic air pollutants including Carbon monoxide (CO), Sulphur dioxide (SO_2), oxides of nitrogen (NO_x), ozone (O_3), Particulate matter, and many others are much higher than the recommended level of WHO's guideline. Furthermore, even with undesirable environmental and health effect of air pollution (HEI 2004), these cities have been incapable to resolve this adverse issue. To reduce emission in major cities several steps have been taken but photochemically produced smog and high level of ozone pose a problem in congested areas.

1.3. Formaldehyde

Despite being the most abundant hydrocarbon in the atmosphere, Formaldehyde (HCHO) has a very short lifetime. Formaldehyde plays a vital role in of the tropospheric. To asses, the emission of non-methane volatile organic compound (NMVOC) and photochemical activity formaldehyde acts an as a key indicator. Fossil fuel combustion and biomass burning primarily emit HCHO.

The prime source of formaldehyde (HCHO) is the oxidation of methane. Half of the global atmospheric HCHO is producing due to this oxidation reaction while the remaining half is being produced during oxidation of NMVOC (Stavrakou *et al.,* 2008). Hence, to bound

and control the NMVOC emissions in chemical transport model satellite measurement of HCHO can be used (Fu *et al.,* 2007).

1.3.1. Tropospheric formaldehyde

In order to monitor the formaldehyde present in the troposphere, UV backscatter satellite sensors are used (Vrekoussis *et al.,* 2010).

1.4. Remote Sensing and DOAS

Measurement of atmospheric gases and other parameter can be done either on small scale by using in situ techniques in which we take a sample or on large scale by remote sensing. In past, remote sensing techniques were developed for military surveillance and reconnaissance purposes, which is still being considered an important tool in the military. In the beginning, remote sensing technique used absorption measurement for the detection of ozone (e.g., Dobson & Harrison, 1926), but with the passage of time, scientist used this technique to enhance their knowledge about atmosphere. Currently, this technique has become a necessary tool in the field of astronomy and environment. Furthermore, ground-based and satellite-based observations are used to assess the global distribution of trace gases and weather conditions.

1.4.1. Active and Passive DOAS:

The Multi-Axis Differential Optical absorption spectrophotometer method has been effectively used for the measurement of many gases including BrO, HCHO, NO_2, SO_2 and CHOCHO (e.g. Cl'emer et al., 2009; Vlemmix et al., 2010, 2011a).

1.5. The Present Study

This study was designed to quantify the formaldehyde concentration in the cities of Rawalpindi and Islamabad. Besides twin cities, the periodic mobile monitoring of HCHO within the cities of Lahore and Multan were also incorporated in this study. For ground-based measurement of formaldehyde MAX-DOAS (Multi-Axis Differential Optical absorption spectrophotometer) instrument was used. The instrument was mounted on rooftop of IESE, sector H-12, Islamabad. For monitoring both in Lahore and Multan, the device was mounted on the rooftop of car. In order to retrieve the differential slant column densities from measured spectra, DOASIS software was used. Then these ground-based results were validated with satellite observations are discussed in detail in the following result and discussion chapter.

1.5.1. Study Area

The study area is located in Islamabad (33°38´ N 72°59´ E). Islamabad is the capital of Pakistan. its elevation from sea level is approximately 450 meters (1827 ft). Islamabad is a mountainous region and is located in Pothwar Pleatue. The climate of Islamabad has a typical version of humid subtropical climate. The city is divided into eight basic sectors, some of which are shown in Fig. 1.1 (F, G, H, and I). Rapid growth in urbanization and advancement in technology put extra stress on natural resources and hence affecting the environment (Sheikh *et al.*, 2007).

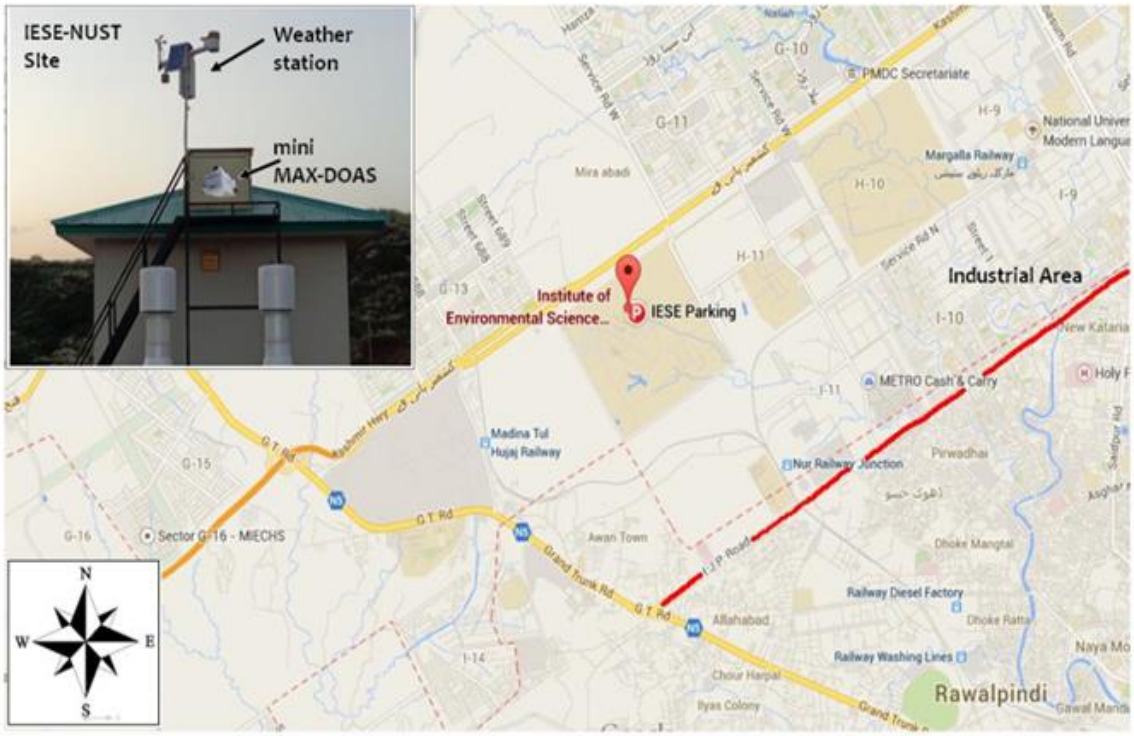

Fig 1.1: Google Map of Study area IESE, Islamabad, Rawalpindi and Vacinity Region

An instrument for monitoring of air pollution was mounted on IESE NUST building. This site is close to Kashmir highway which has a high traffic flux.

1.6. Objectives of the Study

- To monitor the diurnal and weekly cycle of formaldehyde concentration by using MAX-DOAS
- To compare the satellite concentration of formaldehyde with MAX-DOAS measurements

1.7. Importance of Study

As Pakistan is switching its economy from agriculture to industrialization, air pollution and its associated health impacts are also increasing day by day. Therefore, there is an urgent

need to assess the ambient air quality of the region. This study will be helpful to give baseline data of formaldehyde concentration in Islamabad. Furthermore, it will also help in finding some local solutions to counter effects of air pollution on environment and health. This study will also provide the contribution coming from different emission sources, and hence a mitigation measure can be taken accordingly. The Government and Non-Government organization (NGO's) can use this data for making guidelines, Standards, and airport abatement policies. Research institutes can also use this data for their research purposes. Moreover, data of Formaldehyde is not available in Pakistan, hence this will be very beneficial in evaluating the level and possible sources of HCHO. This study can also play an important role in designing techniques that may be useful in order to control air pollution.

Chapter 2

2. Literature Review

2.1. Structure and Composition of the atmosphere

A thin layer of gases known as atmosphere, attracted by the gravity of Earth, separates earth from the outer atmosphere. A prolonged evolutionary process about four and half billion years is responsible for the present condition of the atmosphere (Seinfeld et al., 2012). Carbon dioxide and water vapors mainly emit in the atmosphere due to strong volcanic emissions on earth. Seas and ocean formed when earth got cool and water vapors condensed. Photochemical reactions are the main sources of nitrogen and carbon dioxide in the atmosphere. A large amount of carbon dioxide is converted into oxygen by a microorganism present in the ocean and then plants on land are also the sink of carbon dioxide. The concentration of atmospheric oxygen subsequently elevated permitting the creation of the ozone layer as well as the development of various life forms depending on oxygen for the proper functioning of their metabolic cycle. The table 2.1 shows the compositional structure of current atmosphere.

Table 2.1.: Key constituent of the atmosphere (Wayne 2000)

Constituent	Volume Mixing Ratio
Nitrogen (NO_2)	78.05 %
Oxygen (O_2)	20.95 %
Argon (Ar)	0.93 %
Carbon Dioxide (CO_2)	0.035 %
Water Vapors (H_2O)	0-4 %
Helium (He)	5.5 ppm
Neon (Ne)	18 ppm
Methane (CH_4)	1.7ppm

Nitrogen and oxygen are the important elements of the atmosphere. Because of the triple covalent bond between the nitrogen atoms, nitrogen (N_2) is stable and inert gas. Therefore, oxygen is mostly involved in reactions between substances occurred in the air (Scienfeld and Pandis, 2012). Under standard condition normally those radicals (e.g., OH, NO, NO_2) that have an unpaired electron and tend to react with other molecules is involved. As a result, the short lifetime of radical is between seconds to hours and their concentration is found in a very small range of parts per billion, and highly flexible as depending on different condition includes sunlight, distance to source and reactant availability (Mellouki et al., 2015). In comparison with noble gases which are inert and having a stable mixing ratio, the mixing ratio of water vapors is highly variable as depending on local weather condition (Solomon et al., 2010). The inconsistence uptake and release of carbon dioxide from vegetation cause an increase in carbon dioxide concentration in the atmosphere. Move

over, the anthropogenic activity also increases its concentration. Water vapors, carbon dioxide, and methane are the most important greenhouse gases (Berman et al., 2012).

Atmospheric properties and radiative transfer are largely affected by aerosols. The surface of particles acts as a site for heterogeneous reactions. Transfer of radiation can be observed by eye e.g., dust event and polluted location. Both natural and anthropogenic sources (e.g., volcanoes, biomass burning, industry, sea spray etc.) are responsible for the aerosols formation (Lu et al., 2015).

The below figure 2.1 shows the biochemical cycle in the atmosphere and illustrates that how oceans and continent usually released chemical compounds from their surfaces, how they changed in the atmosphere and how they removed from the atmosphere to be recycled other environmental reservoir of the earth. The bases of a minor compound of the atmosphere are usually situated on the earth surface. After being released into the atmosphere, winds play an important role to transform and transport chemical horizontally and vertically. Impact of the minor compound on different types of geographic and temporal scales depends upon the atmospheric lifetime and concentration of the chemical (Moran et at., 2014). Short-lived compounds pose local impacts while long-lived compounds cause global impacts mostly on climate or on stratospheric ozone. Stratospheric ozone protects the living thing from harmful UV radiation, at the same time ozone present in troposphere is known as greenhouse gas causes severe impact on human health and plants (Bais et al., 2015).

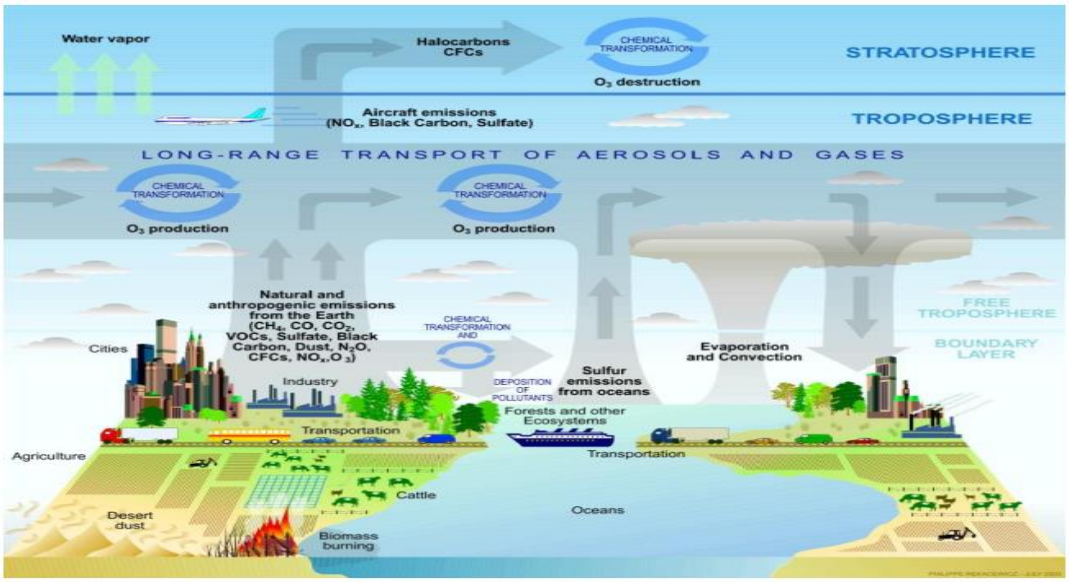

Fig 2.1: Chemicals emissions, transformation, transport and their deposition processes related to atmospheric composition (Moran et al., 2014).

2.2. Atmospheric Structure

2.2.1. Troposphere

This the thinnest and lowest layer of the atmosphere. About 80% atmospheric mass is present in this layer. The adiabatic expansion and compression of rising and sinking of air masses, controlled by solar radiation make it temperature dominant layer. Air is heated and rises during the day when it comes into contact with Earth's surface. It is then cooled via adiabatic expansion leading to the formation of tropopause by a decrease in temperature of 5 -10° per 1 km altitude (Chimonas et al., 1989).

2.2.2. Stratosphere

Ozone absorbs the solar radiation in the upper stratosphere, which leads to an increase in temperature with altitude. In this layer convection and mixing is very little. In comparison

with troposphere, the stratosphere's radiative budget is evaluated by solar radiation absorption and emission of IR radiation.

2.2.3. Mesosphere

The mesosphere is above the stratopause. Like troposphere, the is also decreased in this layer due to a similar process as in the troposphere. In this layer small amount of ozone is present which absorb the thermal radiation.

2.2.4. Thermosphere

In the thermosphere, oxygen strongly absorbs UV radiation leading to a temperature increase of 1200 – 1500 K. The presence of ions and free radicals above the altitude of 50 km characterizes it as ionosphere. At about 100 km, the separation of atmospheric constituents commences with respect to their masses, and when an altitude of 1000 km is reached, the only constituent left is hydrogen. Hence, this region is called heterosphere (Hanslmeier, 2007).

2.3. Formaldehyde

Formaldehyde is one of the most abundant elements in the atmosphere. In the troposphere major portion of formaldehyde concentration comes from chemical degradation of methane and NMVOC (Stavrakou et al., 2009a). Fossil fuels burning and Vegetation fires also contribute a little proportion of formaldehyde in the troposphere (Olivier et al., 2003; Andrea, 2001). Formaldehyde act a proxy or detector of NMVOC photochemical activity that is why oxidation of NMVOC and methane considered as the main source of formaldehyde in air. Despite of very short lifespan ($\tau \approx 3$ hours), HCHO reacts with free radicals and sunlight and plays a very crucial role in of tropospheric chemistry. (Anderson

et al., 1996; Larsen & Larsen, 1998). Due to its short life, CH_2O is removed from the atmosphere by photolysis and reaction with OH radical (Brune *et al.,* 1999). HCHO with a lifetime of 1.5 hours usually produced by the oxidation of volatile organic compound (Sander *et al.,* 2006). Certain substances in the atmosphere do react with HCHO but do not play a major role in its chemistry including Nitrate radicals, hydrogen peroxide, chlorine, ozone and hydroperoxyl radicals (EC, 2001).

The two possible pathways of photolysis to remove formaldehyde during the day, other than wet and dry deposition, are:

- $CO+H_2$ and $CO+2HO_2$
- Oxidation by OH radicals (yielding $CO+HO_2+H_2O$)

Oxidation of methane produced half of the HCHO globally, while the remaing half is produced by oxidation process of NMVOC and some man-made activities (Stavrakou et al., 2008).

2.3.1. Sources

2.3.1.1. Natural Sources

The atmospheric hydrocarbon oxidation is the important natural source of formaldehyde prduction. HCHO is generated as a co-product in the natural methane cycle, with very minor background level. In soil decomposition of plants residue also produce HCHO.

2.3.1.2. Anthropogenic Sources

The anthropogenic sources of formaldehyde include heating, cooking, cigarette smoke and direct emissions. Products containing HCHO include glues, plywood, resins, materials used for insulation, chipboards, and fabrics are the most generic sources.

2.4. Significance and its challenges

Measurement of HCHO is the main serious problem. The concentration of formaldehyde in the air is very low or even in trace amount, and hard to measure formaldehyde accurately. In order to overcome this problem and measure HCHO in its actual concentration, we need a sophisticated and latest equipment. As this oxidation of different VOC cause many other trace gases to measure HCHO in its direct form is very challenging.

2.5. Formaldehyde Occurrence

HCHO is mainly found in urban places exhibited a mixing ratio of 1 to 20 ppb and even more in highly polluted areas because HCHO is produced as a byproduct of oxidation of VOCs [Finlayson-Pitts and Pitts, Jr. 2000]. Fossil fuel combustion and industrial activities are also among the sources of HCHO. The natural sources of Formaldehyde include vegetation which emits isoprene, a precursor of Formaldehyde; and biomass burning. Moreover, HCO is also released in the atmosphere as a by-product of the methane cycle. Methane is abundantly found in the atmosphere and has a lifetime of nine years. Therefore, a constant distribution of HCHO is found in the atmospheric column up to 15 to 20 kilometers [Finlayson-Pitts and Pitts, Jr. 2000].

2.5.1. Formaldehyde in the Atmosphere

HCHO is found in very low background concentrations in the troposphere ranging from 0.02 to 0.2 ppbv (Fried et al., 2008a, b). However, in rural areas, they can reach up to 20 ppbv (Apel et al., 1998; Lee et al., 1998; Choi et al., 2010; Galloway et al., 2011a), and in urban areas, around 45 ppbv (Dasgupta et al., 2005).

2.5.2. Global Formaldehyde Budget

The atmospheric and tropospheric Formaldehyde is influenced by four major sources on a global level i.e. Biomass burning, biogenic emissions, anthropogenic activities and Methane oxidation.

2.6. Formaldehyde in the air

One of the most common aldehydes presents in the troposphere is formaldehyde. The concentration of HCHO present naturally is < 1 μg/m with an average of about 0.5 μg/m (Weber et al 1977). HCHO produced in far areas is usually due to photochemical activity and oxidation of hydrocarbons in these areas (EC, 2001). The range of indoor concentration of formaldehyde is 0.02 to 0.06 mg/m^3. Formaldehyde is also used in construction materials (IARC, 1995).

A small quantity of HCHO in an indoor environment is due to natural and industrial sources. Naturally, O_3 and OH radical react with hydrocarbons in the atmosphere to form formaldehyde. In urban areas, Formaldehyde concentration can range from 1-20 mg/m^3 (WHO, 1989; IARC, 1995).

In cities the most important source of HCHO is the vehicular emission. Incomplete combustion of fuels in vehicles can produce formaldehyde in urban areas and during high traffic load time can reach up to 100 mg/m^3 (WHO, 1989).

2.7. Exposure to formaldehyde

Formaldehyde exposure from construction material, food, fabric and even from ambient air in megacities has been drastically increased. The detectable limit of formaldehyde by human is 0.1 to 0.5 ppm (about 0.12–0.6 mg/m^3), while the range between 0.5 and 1.0 ppm

(0.6–1.2 mg/m^3) can cause eye irritation, and more than 1.0 ppm (1.23 mg/m^3) can irritate the nose and throat (NICNAS, 2006).

2.8. Health Effect of Formaldehyde

The collective effects of ambient, residential, industrial contact to formaldehyde have caused severe health effects. In the past two decades, reports of Formaldehyde exposure have been reported from polluted air, water and food. In the world, the negative health impact of these exposure cases is going up with every passing day.

2.8.1. Acute Toxicity

Acute exposure to HCHO causes acute poisoning results in irritation and immune-toxic effects, irritation of mucous membrane and respiratory tract. Severe inhalation may cause a headache, vomiting, weakness, nausea, pneumonia, and coma. HCHO is corrosive in nature so it may cause skin burn as well (Tang et al., 2009).

2.8.2. Chronic Toxicity

Long-term occupational exposure to Formaldehyde has been known to cause irritation in eyes and in the upper and lower respiratory tracts. In addition, chronic exposure has also been linked to reduced lung function and inflammation of the mucous membranes.

2.8.3. Formaldehyde as Carcinogenic

Studies have also established Formaldehyde as a human carcinogen (Tang et al., 2009). Detailed research and large-scale human studies conducted internationally, formaldehyde was declared as a human carcinogen that causes nasopharyngeal cancer (IARC, 2004).

2.8.4. WHO guidelines and standards for Formaldehyde:

Human health protection is the main purpose to make the main guidelines. In order to protect the human, who has less immunity or are more susceptible to toxic chemical, the standards and guideline are established.

According to the World Health Organization, the concentration of HCHO in the ambient air must be at a level of 100 $\mu g/m^3$, 30-minute exposure on average for all protection. According to another recommendation, its amount in the air should not be above than the 100 g/m^3 retaining at a minimum time ("Concise International Chemical Assessment Document 40", 2002).

2.9. DOAS Spectroscopic Method

DOAS is one of the most extensively used spectroscopic technique in atmospheric research. It is used to classify the concentration of different trace gases in the atmosphere (Piatt & Stutz, 2008). In 1979 platt and his companion introduce this technique. This technique works on the change in absorption at different wavelengths. It measures these trace gases in the Ultra-Violet and Visible region. DOAS can be used to measure the concentration of different trace gases includes HONO, NO_2, BrO, O_3, HCHO, OClO, H_2O and NH_3. Figure 2.2 explains the components of simplified DOAS setup.

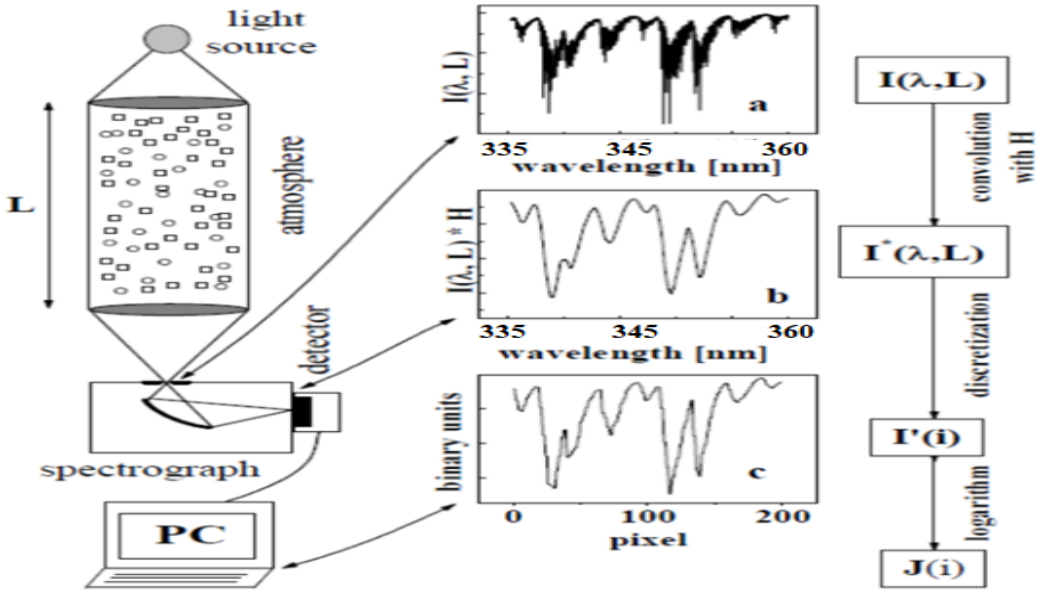

Fig 2.2: The components of a simplified DOAS setup (a) shows the respective spectrum with absorption structure of HCHO (b) convolution of the light was achieved by means of the spectrograph and (c) shows the mapping by the detector (Platt & Stutz, 2008).

By using this technique amounts of trace gases can be retrieved at the same time. It saves monitoring time and allows the analysis of different gases in the observed air mass. Normally, there are two types of DOAS. Those who use artificial light source are called

active, while those who use natural light as their light source (e.g. Solar Radiations) are known as passive.

The basic working principal of DOAS technique is based on “Lambert beer Law”, which states the linear relationship between light and matter. According to this law, the absorption of light is directly proportional to the path length and concentration of the analyte. In other word compare the incoming radiation ($I0_\lambda$) with outgoing (I_λ) by a function of path length (L) of the light and the concentration (c) and absorption cross-section (σ_λ) of the species in the equation mentioned below:

$$I_\lambda = I_{0\,\lambda}.\, e^{-L\sigma(\lambda)\, c}$$

This relationship can be used to calculate the concentration of a trace gas by setting up a light source of known spectral intensity and a sensor at some distance (L). The pectoral demonstration of working principle is given in figure 2.3 given below.

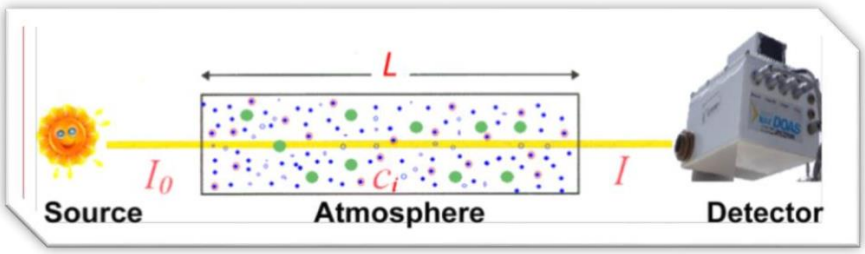

Fig 2.3: Illustration of DOAS Principle

2.10. Satellite Observation

Ozone Monitoring Instrument (OMI) has a high spectral resolution and has the ability to measure several trace gases in the UV/Vis wavelength range for the same air mass. It is an instrument of the European Global Ozone Monitoring Experiment (GOME).

2.10.1. OMI's Spectral Channels

The spectral range in which reflected light is observed by Ozone Monitoring Instrument (OMI) is usually laid between Ultra-Violet to Visible (i.e. 270nm – 500nm). With a spectral resolution of 0.5nm OMI in two channels. Ultra-Violet Channel is further divided into two subchannels UV-1 (270-310nm) and UV-2 (310-365NM).

Chapter 3

3. Material and Method

3.1. Instrument Mini-Max DOAS:

The Multi Axis-Differential Optical Absorption Spectroscopy (MAX-DOAS) is a highly sophisticated lightweight device that can be used both for stationary and mobile monitoring of trace gases. It is specially designed in order to monitor the backscattered sunlight. Fiber spectrograph and some other controlling electronic parts are tightly closed in an aluminum box. A stepper motor is used to move the instrument at different elevation angle (Precision = 0.1 degree/step, Frequency= 784Hz). At the optics entrance, there exists a quartz lens with a focal length of 40mm. The spectral range is detected by a "Czerny Turner Spectrometer (Ocea Optics Inc., USB-2000+). For continuous ground-based monitoring, the detectable range of spectrometer was 318-465 nm having a spectral resolution equals to 0.7nm, while for the periodic field measurement, the spectral resolution of the device was 305-470nm and the remaining configurations were kept the same.

Having 2048 pixels, the portable instrument (coupled charged device 1 dimensional-CCD) was employed as a detector, which uses Peltier cooling (Thermoelectric cooling) as a means to regulate the internal temperature. Furthermore, to store and acquire the data, a computer system was continuously running with windows XP and DOASIS software installed.

Figure 3.1: Mini Max- DOAS Instrument

3.2. Monitoring Sites and Schedule

During this research two instruments was used for the measurement of formaldehyde. One instrument was deployed at IESE, NUST, Islamabad sampling site for the continuous monitoring, while the second instrument was used for periodic field campaigns. Further detail of ground-based and field samplings is briefly given in table 3.1 below.

Table 3.1: Ground-based and Field Campaign schedule and other detail.

Activity Detail	Location	Dates
* GM: Continuous Ground Monitoring at Islamabad	Islamabad	1st September 2015 – 31st August 2017
** FC-1: Max DOAS Field Campaign	Lahore	18th December 2015
FC-2: 1st Round (morning to noon) Around Lahore Ring Road	Lahore	2nd January 2016

2nd Round (afternoon to evening) Around Lahore Ring Road		
FC-3: 1st Round (morning to noon) Around Lahore Ring Road 2nd Round (afternoon to evening) Around Lahore Ring Road	Lahore	15th January 2016
FC-4: Within and around Lahore	Lahore	2nd February 2016
FC-5: 1st Round (morning to noon) Around Lahore Ring Road 2nd Round (afternoon to evening) Around Lahore Ring Road	Lahore	20th February 2016
FC-6: 1st Round (morning to noon) Around Lahore Ring Road 2nd Round (afternoon to evening) Around Lahore Ring Road	Lahore	21st February 2016
FC-7: 1st Round (morning to noon) Around Lahore Ring Road 2nd Round (afternoon to evening) Around Lahore Ring Road	Lahore	27th December 2016
FC-8: Within and around Multan	Multan	28th December 2016
FC-9: Within and around Multan	Multan	29th December 2016
FC-10: Within and around Lahore	Lahore	14th January 2017
FC-11: Within and around Multan	Multan	15th January 2017
FC-12: Within and around Lahore	Lahore	3rd February 2017
FC-13: Within and around Multan	Multan	4th February 2017
FC-14: Within and around Lahore	Lahore	26th February 2017
FC-13: Within and around Multan	Multan	27th February 2017

FC-14: Within and around Islamabad-Rawalpindi	Islamabad - Rawalpindi	2nd March 2017

**FC=Field campaigns, *GM=Ground Monitoring

For field campaign, three megacities of Punjab (Lahore, Multan, and Islamabad) were selected. In Lahore ring road, in twin cities Kashmir highway, G.T road and Express highway, while in Multan, Multan bypass was selected for the campaign. Two rounds in a day were conducted, the first round was started at early morning and second round was started in afternoon. During field campaign, the elevation viewing angle was used one 90^o and followed by four 30^o (i.e. 90^o, 30^o, 30^o, 30^o). The monitoring time (Tini) at one angle was 60,000-mile sec/scan. The main reason for setting high elevation angles 90^o is to avoid the blockage from building and vehicles, while 30^o angles were used, just because air mass factor (AMF) can be easily calculated at this angle (Wagner *et al.,* 2010). The elevation angle setting for fixed monitoring at IESE, NUST, the site was (2^o, 4^o, 5^o, 10^o, 15^o, 30^o, 45^o, 60^o).

3.3. Software Used during this Study

Start from data acquisition, analyzing than plotting a graph of formaldehyde different software were used, which listed below in table (3.2).

Table 3.2: Softwares and their purpose for use in Research Work

Sr. #	Software	Purpose
1	DOASIS (Differential Optical Absorption Spectroscopy Intelligent System) (v 3.2.35)	Operating Software for MAX-DOAS and measurement of back scatter intensities
2	WinDOAS (Windows Differential Optical Absorption Spectroscopy)	Calibration process is performed.
3	QDOAS (v. 2.111.1)	Analysis of UV-Visible spectra to retrieve DSCDs
4	Microsoft Excel (v. 2016)	Mathematical Calculations for tropospheric VCD extraction and Graphical representations
5	ArcGIS (v. 10.3.1)	Interpolation of OMI Data and Validation of MAX-DOAS data with satellite observations

3.4. DOASIS

DOAS intelligent system is a software, mainly used to operate the Max-DOAS instrument. DOASIS plays many important roles, which includes data retrieval, controlling the stepper motor that is used for moving instrument at different elevation angles, regulate the temperature of the instrument by setting Peltier and spectrum integration time. This software runs on java coded script that gives all necessary command to the software. To calibrate the instrument dark current and offset were taken manually and automatically as coded in the script. The DOASIS software is also used to calculate ring spectrum. Both

ring spectrum and OSDC (Offset Dark current) are used during the analysis of data in QDOAS.

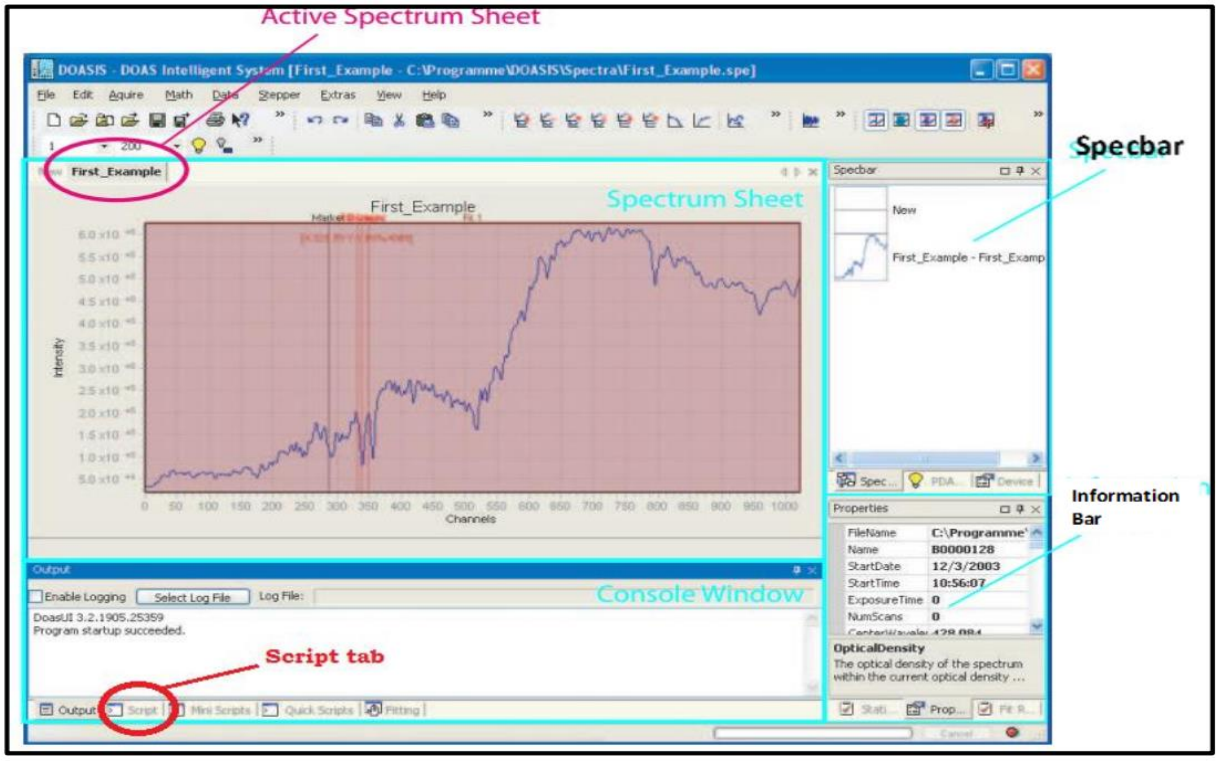

Figure 3.2: DOAS Intelligent System Software Interface

3.4.1. Dark Current

This small electric current is normally measured in the photosensitive instrument (e.g., Spectrometer). For dark current monitoring long exposure time and less number of scan is required.

3.4.2. Offset

The offset is taken in dark condition, in other words “in the absence of photon”. For offset measurement, small exposure and a greater number of scans are required.

Table 3.3: Values required to take OSDC

	Integration/ Exposure time (milliseconds)	Number of Scans
Dark Current	~1	10000
Offset	~100	1000

3.5. Analysis of Formaldehyde

Three main steps were used in the analysis of retrieved trace gases:

i. Wavelength Calibration

ii. Wavelength Convolutions

iii. HCHO Analysis Window

3.5.1. Wavelength Calibration

Window differential optical absorption spectrometer (WinDOAS) software was used to calibrate the wavelength. At noontime (11:30 – 12:30) the high concentration spectrums at 90^{o} having least solar zenith angle (SZA) were taken, mostly used for calibration. The fit was applied between retrieved spectra and convoluted spectra to perform the calibration. Throughout the process, the wavelength of solar spectra was assigned to the single detector's pixels. The calibration fit is also known as "Kurucz-fit". To perform and analyze the fit, wavelength range was divided into sub-windows (6 Sub-windows).

In order to adjust and shift of the spectra between measured and convoluted spectrum "shift and squeeze" option was applied in the calibration process. The polynomial degree was used in Slit function parameter. The Slit function is used to interpolate the result of sub-

windows. Repetition of calibration process usually minimizes the residual process. Using the calibration file against a reference spectrum, all measured spectra are being evaluated.

3.5.2. Wavelength Convolution:

Convolution is a mathematic method, which is important in wavelength processing operations. In QDOAS software "convolution tool" option was used to execute the convolution. There are two types of convolution.

3.5.2.1. Online Convolution

In this type of convolution, the cross sections without any pre-processing are simply inserted in HCHO analysis windows. Because in this convolution, cross sections are automatically convoluted during analysis of spectra.

3.5.2.2. Offline Convolution

In offline type, the cross sections are convoluted before inserting them in analysis windows. In a current study, the online convolution of cross sections was used.

3.5.2.3. Cross Section

The cross sections of different trace gases used in the convolution process with their convolution specifications are listed in table 3.4.

Table 3.4: Cross sections of different trace gases with their convolution specifications

Sr. #	Cross Section	Convolution
1	hcho_297K_Meller	Standard Convolution
2	o4_thalman_volkamer_293K_inAir	Interpolate
3	bro_223K_Fleischmann	Standard Convolution
4	no2_298K_vanDaele	Convolve Io (1e17 molecule/cm^2)
5	o3_223K_SDY_air	Convolve Io (1e20 molecule/cm^2)
6	o3a_243p223K_SDY_336-359nm	Convolve Io (1e20 molecule/cm^2)
7	Ring (Ring_QDOAScalc_HighResSAO_Norm)	Ring Convolution

The cross-section having a high resolution is convoluted by "Standard convolution" (Convolve Std) option. In addition to this option, slit function type Gaussian (FWHM = 0.5nm) and calibration file that is generated in wavelength calibration step were also used. While to evaluate the optical depth in convolution "I_0 correction" (Convolve I_0) option was used (Fayt *et al.,* 2013).

3.5.3. HCHO Analysis

analysis of CH_2O is performed in QODAS software. For analysis of HCHO, different parameters (date, time, SZA and EVA) were selected and check analysis fit block from display option as shown in figure 3.3.

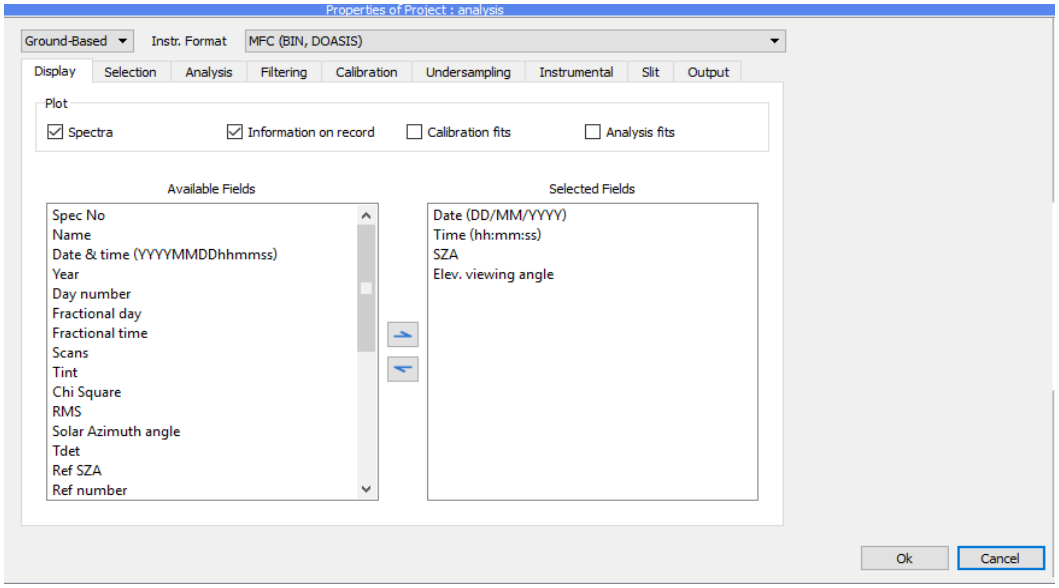

Figure3.3: Display Tab Properties of DOASIS software

Than OSDC, detector size (2048) and calibration file is put in instrumental Tab as shown in figure 3.4. This 2048 is the instrument specific pixel value, that we put manually in the software.

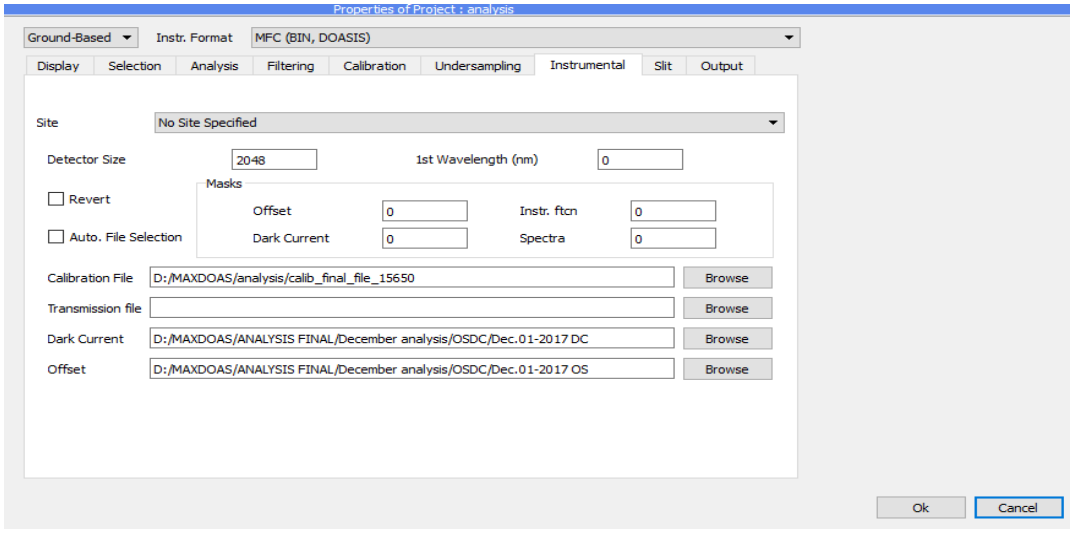

Figure 3.4: Instrumental tab Properties of DOASIS software

Then opened the analysis window and fitting length of formaldehyde was set to 336.5-359nm. All the cross sections their convolution setting was inserted in “Molecules Tab” as shown in figure 3.5. The polynomial degree 0.5 was used for HCHO analysis.

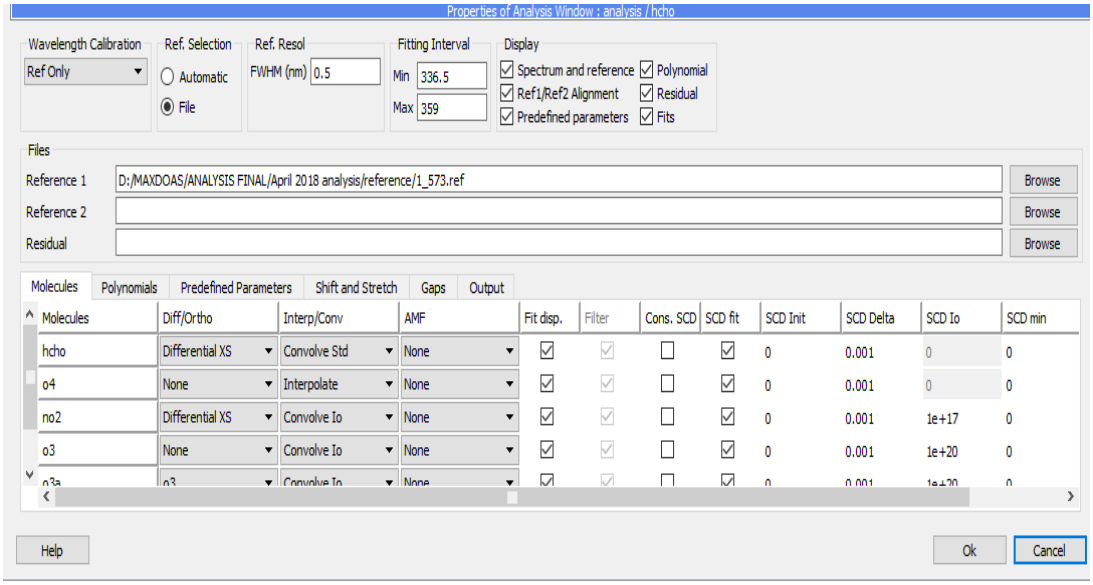

Figure 3.5: Analysis window in QDOAS, showing the fitting interval used for HCHO

The required parameters (RMS, SZA, EVA and time etc.) for results were then selected and output path for the result file was given in “Output Tab”. The analysis was performed on all retrieved spectra and HCHO DSCDs and results were generated in ASCII format file. These results file is then opened in Microsoft Excel, which contains all selected parameters and DSCDs and error of all trace gases as shown in fig 3.6.

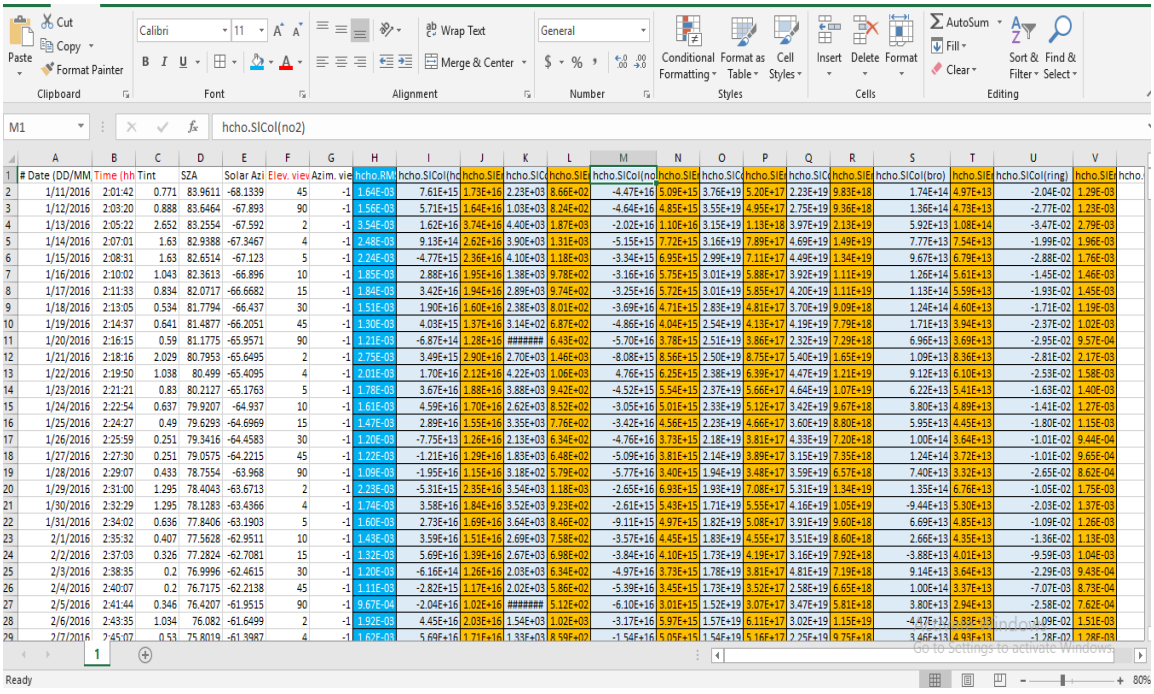

#	Date (DD/MM	Time (hh	Tint	SZA	Solar Azi	Elev. viev	Azim. vie	hcho.RM	hcho.SICol(hc	hcho.SIE	hcho.SIC	hcho.SIE	hcho.SICol(no	hcho.SIE	hcho.SIC	hcho.SIE	hcho.SIC	hcho.SIE	hcho.SICol(bro)	hcho.SIE	hcho.SICol(ring)	hcho.SIE	hcho.
2	1/11/2016	2:01:42	0.771	83.9611	-68.1339	45	-1	1.64E-03	7.61E+15	1.73E+16	2.23E+03	8.66E+02	-4.47E+16	5.09E+15	3.76E+19	5.20E+17	2.23E+19	9.83E+18	1.74E+14	4.97E+13	-2.04E-02	1.29E-03	
3	1/12/2016	2:03:20	0.888	83.6464	-67.893	90	-1	1.56E-03	5.71E+15	1.64E+16	1.03E+03	8.24E+02	-4.64E+16	4.85E+15	3.55E+19	4.95E+17	2.75E+19	9.36E+18	1.36E+14	4.73E+13	-2.77E-02	1.23E-03	
4	1/13/2016	2:05:22	2.652	83.2554	-67.592	2	-1	3.54E-03	1.62E+16	3.74E+16	4.40E+03	1.87E+03	-2.02E+16	1.10E+16	3.15E+19	1.13E+18	3.97E+19	2.13E+19	5.92E+13	1.08E+14	-3.47E-02	2.79E-03	
5	1/14/2016	2:07:01	1.63	82.9388	-67.3467	4	-1	2.48E-03	9.13E+14	2.62E+16	3.90E+03	1.31E+03	-5.15E+15	7.72E+15	3.16E+19	7.89E+17	4.69E+19	1.49E+19	7.77E+13	7.54E+13	-1.99E-02	1.96E-03	
6	1/15/2016	2:08:31	1.63	82.6514	-67.123	5	-1	2.24E-03	-4.77E+15	2.36E+16	4.10E+03	1.18E+03	-3.34E+15	6.95E+15	2.99E+19	7.11E+17	4.49E+19	1.34E+19	9.67E+13	6.79E+13	-2.88E-02	1.76E-03	
7	1/16/2016	2:10:02	1.043	82.3613	-66.896	10	-1	1.85E-03	2.88E+16	1.95E+16	1.38E+03	9.78E+02	-3.16E+16	5.75E+15	3.01E+19	5.88E+17	3.92E+19	1.11E+19	1.26E+14	5.61E+13	-1.45E-02	1.46E-03	
8	1/17/2016	2:11:33	0.834	82.0717	-66.6682	15	-1	1.84E-03	3.42E+16	1.94E+16	2.89E+03	9.74E+02	-3.25E+16	5.72E+15	3.01E+19	5.85E+17	4.20E+19	1.11E+19	1.13E+14	5.59E+13	-1.93E-02	1.45E-03	
9	1/18/2016	2:13:05	0.534	81.7794	-66.437	30	-1	1.51E-03	1.90E+16	1.60E+16	2.38E+03	8.01E+02	-3.69E+16	4.71E+15	2.83E+19	4.81E+17	3.70E+19	9.09E+18	1.24E+14	4.60E+13	-1.71E-02	1.19E-03	
10	1/19/2016	2:14:37	0.641	81.4877	-66.2051	45	-1	1.30E-03	4.03E+15	1.37E+16	3.14E+02	6.87E+02	-4.86E+16	4.04E+15	2.54E+19	4.13E+17	4.19E+19	7.79E+18	1.71E+13	3.94E+13	-2.37E-02	1.02E-03	
11	1/20/2016	2:16:15	0.59	81.1775	-65.9571	90	-1	1.21E-03	-6.87E+14	1.28E+16	#######	6.43E+02	-5.70E+16	3.78E+15	2.51E+19	3.86E+17	2.32E+19	7.29E+18	6.96E+13	3.69E+13	-2.95E-02	9.57E-04	
12	1/21/2016	2:18:16	2.029	80.7953	-65.6495	2	-1	2.75E-03	3.49E+15	2.90E+16	2.70E+03	1.46E+03	-8.08E+15	8.56E+15	2.50E+19	8.75E+17	5.40E+19	1.65E+19	1.09E+13	8.36E+13	-2.81E-02	2.17E-03	
13	1/22/2016	2:19:50	1.038	80.499	-65.4095	4	-1	2.01E-03	1.70E+16	2.12E+16	4.22E+03	1.06E+03	4.76E+15	6.25E+15	2.38E+19	6.39E+17	4.47E+19	1.21E+19	9.12E+13	6.10E+13	-2.53E-02	1.58E-03	
14	1/23/2016	2:21:21	0.83	80.2127	-65.1763	5	-1	1.78E-03	3.67E+16	1.88E+16	3.88E+03	9.42E+02	-4.52E+15	5.54E+15	2.37E+19	5.66E+17	4.64E+19	1.07E+19	6.22E+13	5.41E+13	-1.63E-02	1.40E-03	
15	1/24/2016	2:22:54	0.637	79.9207	-64.937	10	-1	1.61E-03	4.59E+16	1.70E+16	2.62E+03	8.52E+02	-3.05E+16	5.01E+15	2.33E+19	5.12E+17	3.42E+19	9.67E+18	3.80E+13	4.89E+13	-1.41E-02	1.27E-03	
16	1/25/2016	2:24:27	0.49	79.6293	-64.6969	15	-1	1.47E-03	2.89E+16	1.55E+16	3.35E+03	7.76E+02	-3.42E+16	4.56E+15	2.23E+19	4.66E+17	3.60E+19	8.80E+18	5.95E+13	4.45E+13	-1.80E-02	1.15E-03	
17	1/26/2016	2:25:59	0.251	79.3416	-64.4583	30	-1	1.20E-03	-7.75E+13	1.26E+16	2.13E+03	6.34E+02	-4.76E+16	3.73E+15	2.18E+19	3.81E+17	4.33E+19	7.20E+18	1.00E+14	3.64E+13	-1.01E-02	9.44E-04	
18	1/27/2016	2:27:30	0.251	79.0575	-64.2215	45	-1	1.22E-03	-1.21E+16	1.29E+16	1.83E+03	6.48E+02	-5.09E+16	3.81E+15	2.14E+19	3.89E+17	3.15E+19	7.35E+18	1.24E+14	3.72E+13	-1.01E-02	9.65E-04	
19	1/28/2016	2:29:07	0.433	78.7554	-63.968	90	-1	1.09E-03	-1.95E+16	1.15E+16	3.18E+02	5.79E+02	-5.77E+16	3.40E+15	1.94E+19	3.48E+17	3.59E+19	6.57E+18	7.40E+13	3.32E+13	-2.65E-02	8.62E-04	
20	1/29/2016	2:31:00	1.295	78.4043	-63.6713	2	-1	2.23E-03	-5.31E+15	2.35E+16	3.54E+03	1.18E+03	-2.65E+16	6.93E+15	1.93E+19	7.08E+17	5.31E+19	1.34E+19	1.35E+14	6.76E+13	-1.05E-02	1.75E-03	
21	1/30/2016	2:32:29	1.295	78.1283	-63.4366	4	-1	1.74E-03	3.58E+16	1.84E+16	3.52E+03	9.23E+02	-2.61E+15	5.43E+15	1.71E+19	5.55E+17	4.16E+19	1.05E+19	-9.44E+13	5.30E+13	-2.03E-02	1.37E-03	
22	1/31/2016	2:34:02	0.636	77.8406	-63.1903	5	-1	1.60E-03	2.73E+16	1.69E+16	3.64E+03	8.46E+02	-9.11E+15	4.97E+15	1.82E+19	5.08E+17	3.91E+19	9.60E+18	6.69E+13	4.85E+13	-1.09E-02	1.26E-03	
23	2/1/2016	2:35:32	0.407	77.5628	-62.9511	10	-1	1.43E-03	3.59E+16	1.51E+16	2.69E+03	7.58E+02	-3.57E+16	4.45E+15	1.83E+19	4.55E+17	3.51E+19	8.60E+18	2.66E+13	4.35E+13	-1.36E-02	1.13E-03	
24	2/2/2016	2:37:03	0.326	77.2824	-62.7081	15	-1	1.32E-03	5.69E+16	1.39E+16	2.67E+03	6.98E+02	-3.84E+16	4.10E+15	1.73E+19	4.19E+17	3.16E+19	7.92E+18	-3.88E+13	4.01E+13	-9.59E-03	1.04E-03	
25	2/3/2016	2:38:35	0.2	76.9996	-62.4615	30	-1	1.20E-03	-6.16E+14	1.26E+16	2.03E+03	6.34E+02	-4.97E+16	3.73E+15	1.78E+19	3.81E+17	4.81E+19	7.19E+18	9.14E+13	3.64E+13	-2.29E-03	9.43E-04	
26	2/4/2016	2:40:07	0.2	76.7175	-62.2138	45	-1	1.11E-03	-2.82E+15	1.17E+16	2.02E+03	5.86E+02	-5.39E+16	3.45E+15	1.73E+19	3.52E+17	2.58E+19	6.65E+18	1.00E+14	3.37E+13	-7.07E-03	8.73E-04	
27	2/5/2016	2:41:44	0.346	76.4207	-61.9515	90	-1	9.67E-04	-2.04E+16	1.02E+16	#######	5.12E+02	-6.10E+16	3.01E+15	1.52E+19	3.07E+17	3.47E+19	5.81E+18	3.80E+13	2.94E+13	-2.58E-02	7.62E-04	
28	2/6/2016	2:43:35	1.034	76.082	-61.6499	2	-1	1.92E-03	4.45E+16	2.03E+16	1.54E+03	1.02E+03	-3.17E+16	5.97E+15	1.57E+19	6.11E+17	3.02E+19	1.15E+19	-4.47E+12	5.83E+13	-1.09E-02	1.51E-03	
29	2/7/2016	2:45:07	0.53	75.8019	-61.3987	4	-1	1.62E-03	5.69E+16	1.71E+16	1.33E+03	8.59E+02	-1.54E+16	5.05E+15	1.54E+19	5.16E+17	2.25E+19	9.75E+18	3.46E+13	4.93E+13	-1.28E-02	1.28E-03	

Figure 3.6: ASCII files obtained by QDOAS opened in Microsoft Excel; blue column representing RMS, gray columns showing DSCDs, yellow columns illustrate slant column errors

3.6. Calculation of DAMF and Tropospheric VCD

The Air Mass Factor is a ratio of solar radiation path length coming directly from the atmosphere to coming vertically through the atmosphere, mathematically DAMF is defined as a difference of AMF between $\alpha \neq 90°$ and $\alpha = 90°$, where $\propto$ is elevation angle. Microsoft Excel software was used to calculate air mass factor because this software is convenient to drive the VCD. The calculation of VCDs from stationary mobile data is different from mobile data. If the last dissipating event of energy packets (photon) been recorded by the instrumental telescope occurs higher than the layer of gas, the AMF for zenith and off-axis view can be evaluated as 1 (sin 90°=1) and 1/sinα, respectively (Li *et al.*, 2012).

$$\mathbf{DAMF\alpha = (1/\ sin\alpha) - 1}$$

As AMF is a ratio of slant column densities to vertical column densities, so VCD is derived from AMF by converting it into DSCD than into VCD. the AMF for zenith and off-axis view can be evaluated as 1 (sin 90°=1) and 1⁄sinα, respectively (Li *et al.*, 2012).

$$\mathbf{VCD = DSCD\ (\alpha) / DMAF(\alpha)\ \text{------}\ Eq.\ 1}$$

$$\mathbf{VCD = DSCD\ (\alpha) / (1/\ sin\alpha) - 1\text{------}\ Eq.\ 2}$$

Where, α = Elevation Angle and geo = Geometric Approach. In the current study, for HCHO VCD for a corresponding DSCD at the off-zenith elevation angle, i.e. α = 30◦ was used for both ground and field campaign.

3.7. Projection of Field Campaigns VCD

The map of Vertical Column Densities (VCD) HCHO from Lahore and Multan were plotted as per their coordinate of measurement. We used a GPS device to measure the latitude and longitude of the whole campaign route. Then the VCD values were put against correspondent latitude and longitude by matching the time of both GPS logger and Max-DOAS device reading and save the file in CSV (comma delimited) format. In the next step. This CSV file was opened in ArcMap (version 10.3.1) and mapped the VCDs as shown in Figure 3.7.

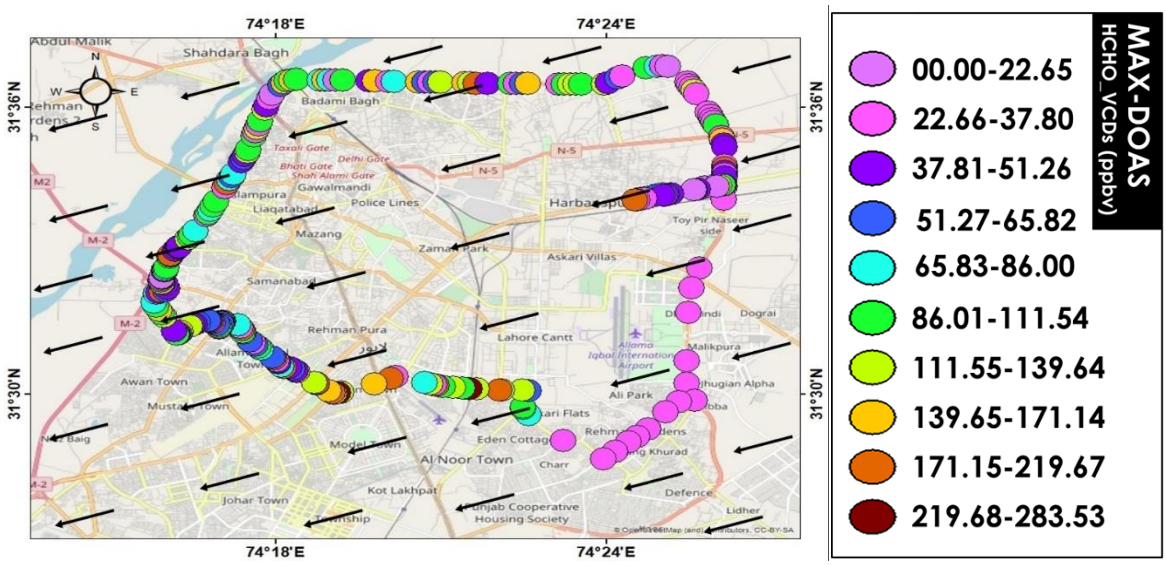

Figure 3.7: HCHO field campaign map and legend generated by ArcGIS. The black arrows on map represents the wind direction

3.8. Validation of Ground-Based and Satellite-Based Data

For the validation purpose, the comparison of ground-based (IESE-NUST) with satellite data was carried out. The HCHO satellite was taken from ozone monitoring instrument (OMI - Boersma *et la.*, 2007). The specifications of the ozone monitoring instrument are given in Table 3.4.

Table 3.4: Specifications of ozone monitoring instrument

Instrument	OMI
Platform	AURA
Measurement Period	2004-2016
Equator crossing time	13:40 – 13:50
Spatial Resolution	24*13
Spectral Resolution	0.5
Spectral Region	UV-Vis
Global Coverage	1 Day
Grid Size	0.25*0.25

Level-3 OMI HCHO tropospheric VCD product from TEMIS was used in this study, established by scientific developments performed at BIRA. The link of the data source is (http://h2co.aeronomie.be/ch2o/ch2o.php?instr=omi&period=month). The different software used in satellite data processing include

- ENVI +IDL 5.0
- ArcMap 10.3.1 for mapping

The monthly and daily data (for field campaigns' days only) of HCHO was download in ASCII format. Than ENVI +IDL 5.0 was used to make raster. This raster is then opened in ArcMap to make it georeferenced. Islamabad, Lahore and Multan's shapefile were used to extract VCDs and produce spatial maps of these cities from global data.

Chapter 4

4. Results and Discussion

4.1. Observation of HCHO during Field Campaigns

The periodic measurements of HCHO VCDs were carried out by using MAX-DOAS instrument on rooftop of a car were performed within and around the boundary of Lahore, Multan, and Islamabad-Rawalpindi during the period of 18th December 2015 to 3rd March 2017 as mentioned in the table 4.1 below Respectively. ArcMap 10.3.1 was used to plot the HCHO VCDs (ppb) for all the cities as shown in figure 4.1 respectively.

4.1.1. Field Campaigns around Lahore City

In Lahore, the maximum value of HCHO was found during the second trip on 6th November, 2016 with 3.31 x 10^{17} molecules/cm^2 (283.5 ppbv) near the airport road. This high concertation is due to the burning of fossil fuel and agriculture residues because smog episode happened during the first week of November 2016. The second and third highest concentration of HCHO in Lahore were calculated in round 2 near Thokar Niaz Baig and in round 1 near Ring Road Industrial area on 2nd January and 2nd February, 2017 respectively. The values of above-mentioned concentrations were 1.93 x 10^{17}(164.33 ppbv) molecules/cm^2 and 1.28 x 10^{17}(108.99 ppbv) molecules/cm^2 respectively. The possible reasons for such high concentrations could be due to of traffic jam and industrial emissions. All three concentrations are exceeding the WHO permissible limit for HCHO in ambient air (83 ppbv, WHO Report 1989).

Table 4.1.: Maximum and average Concentrations of HCHO over Lahore observed during Field Campaigns

Location	Date	Distance (km)	Avg._NO_2 VCD (molec/cm^2)	Max_NO_2 VCD (molec/cm^2)	Max_NO_2 VCD (ppbv)
Lahore	18-December 2015	81.3	1.15E+16	2.27E+16	19.33
Lahore (R1)	02-Jan-2016	93.3	8.96E+15	2.85E+16	24.27
Lahore (R2)	02-Jan-2016	81.6	3.13E+16	1.93E+17	**164.33**
Lahore (R1)	15-Jan-2016	72.3	9.20E+15	3.38E+16	28.78
Lahore (R2)	15-Jan-2016	75.3	2.51E+16	7.49E+16	63.77
Lahore	02-Feb-2016	82	5.63E+16	1.28E+17	**108.99**
Lahore (R1)	20-Feb-2016	88	1.31E+16	2.96E+16	25.20
Lahore (R2)	20-Feb-2016	74.4	1.48E+16	3.29E+16	28.01
Lahore (R1)	21-Feb-2016	82.3	1.53E+16	2.59E+16	22.05
Lahore (R2)	21-Feb-2016	74.3	1.23E+16	6.81E+16	57.98
Lahore	05-Nov-2016	65	1.80E+16	2.86E+16	24.35
Lahore (R1)	06-Nov-2016	72.81	2.34E+16	3.44E+16	29.29
Lahore (R2)	06-Nov-2016	78.76	1.02E+17	3.33E+17	**283.53**
Lahore (R1)	07-Nov-2016	68.1	1.86E+16	3.19E+16	27.16
Lahore (R2)	07-Nove-2016	57.50	2.48E+16	3.97E+16	33.80
Lahore (R1)	27-Dec-2016	74.79	2.07E+16	5.87E+16	49.98

Lahore (R2)	27-December 2016	69.25	2.23E+16	5.94E+16	50.58
Lahore	14-January 2017	65.38	1.41E+16	3.13E+16	26.65
Lahore	03-February 2017	72.76	2.36E+16	5.00E+16	42.57
Lahore	26-February 2017	66.30	1.81E+16	2.89E+16	24.61

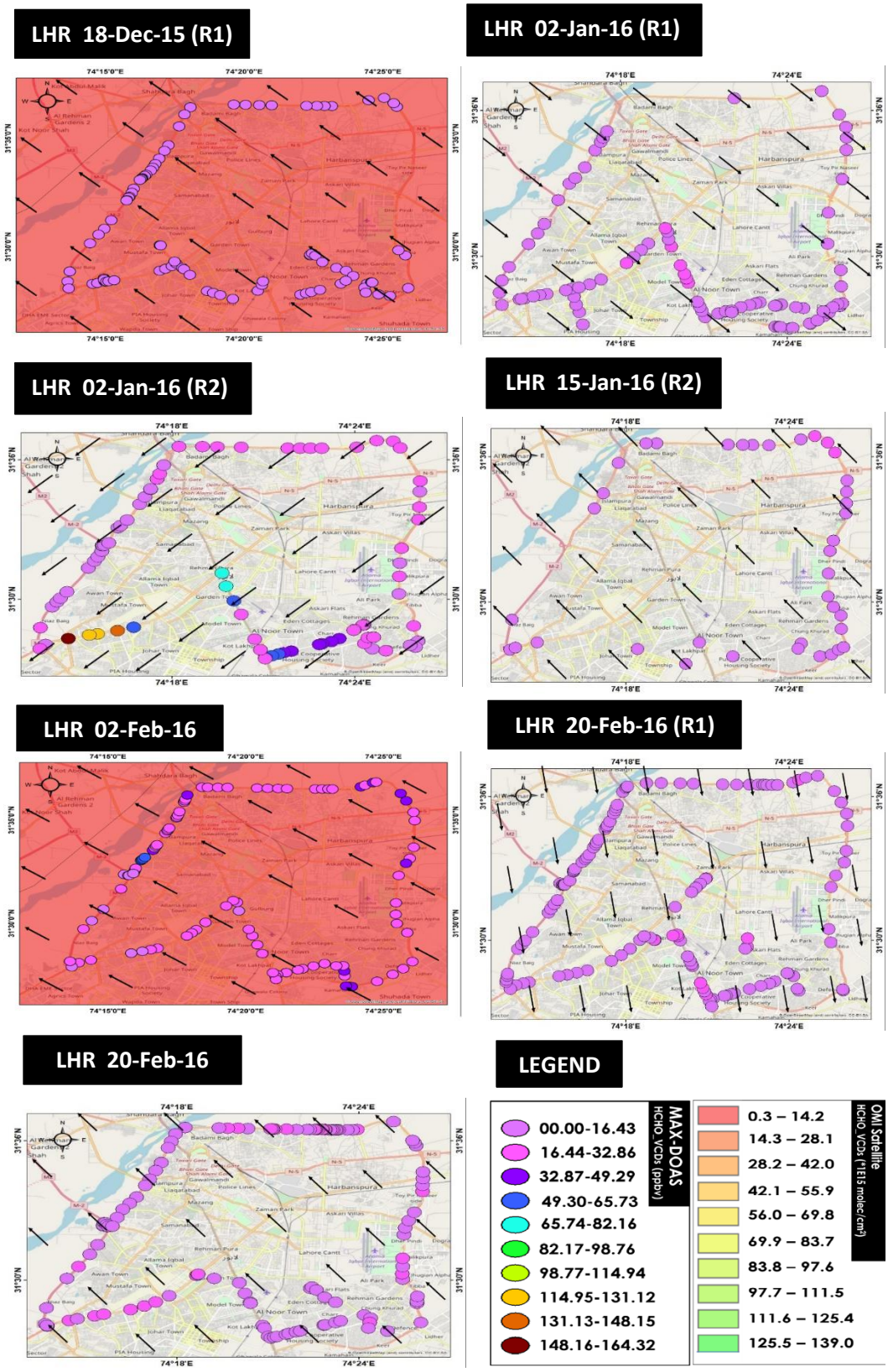

Fig 4.1: HCHO concentrations with legend retrieved from car MAX-DOAS and OMI satellite observations conducted in the city of Lahore. Wind vectors are also included to represent the average wind direction during that field campaign observations.

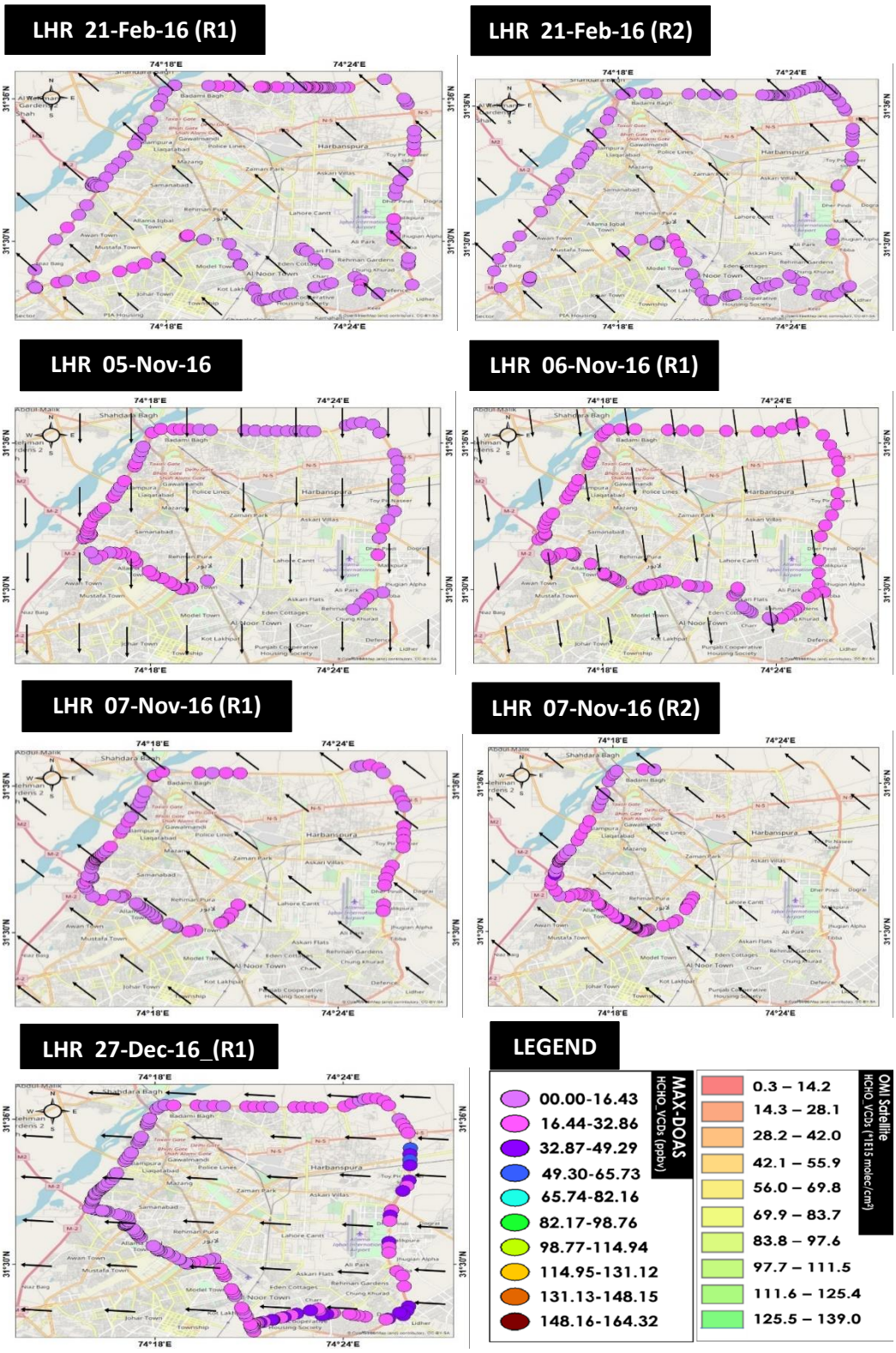

Fig 4.1: HCHO concentrations with legend retrieved from car MAX-DOAS and OMI satellite observations conducted in the city of Lahore. Wind vectors are also included to represent the average wind direction during that field campaign observations.

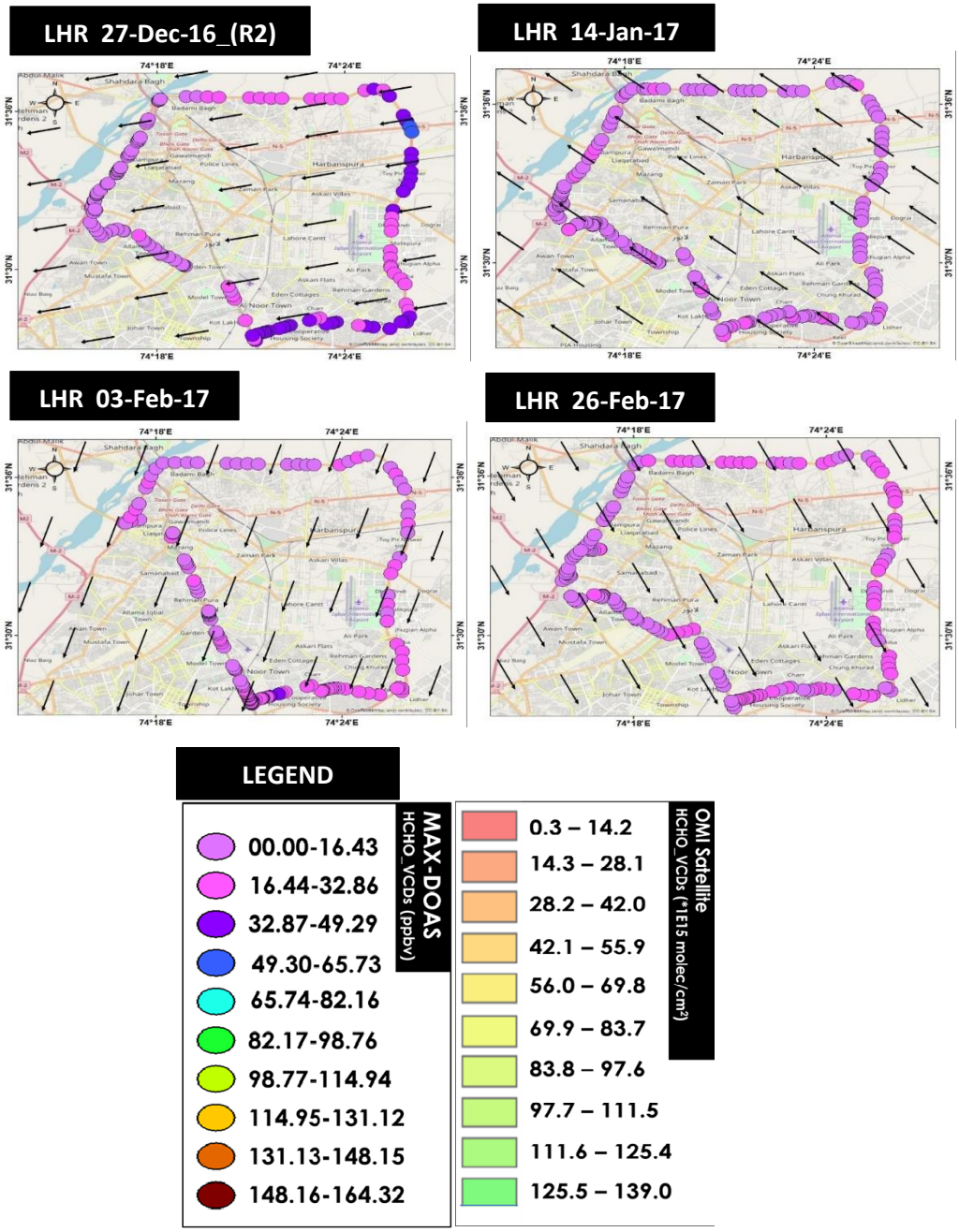

Fig 4.1: HCHO concentrations with legend retrieved from car MAX-DOAS and OMI satellite observations conducted in the city of Lahore. Wind vectors are also included to represent the average wind direction during that field campaign observations.

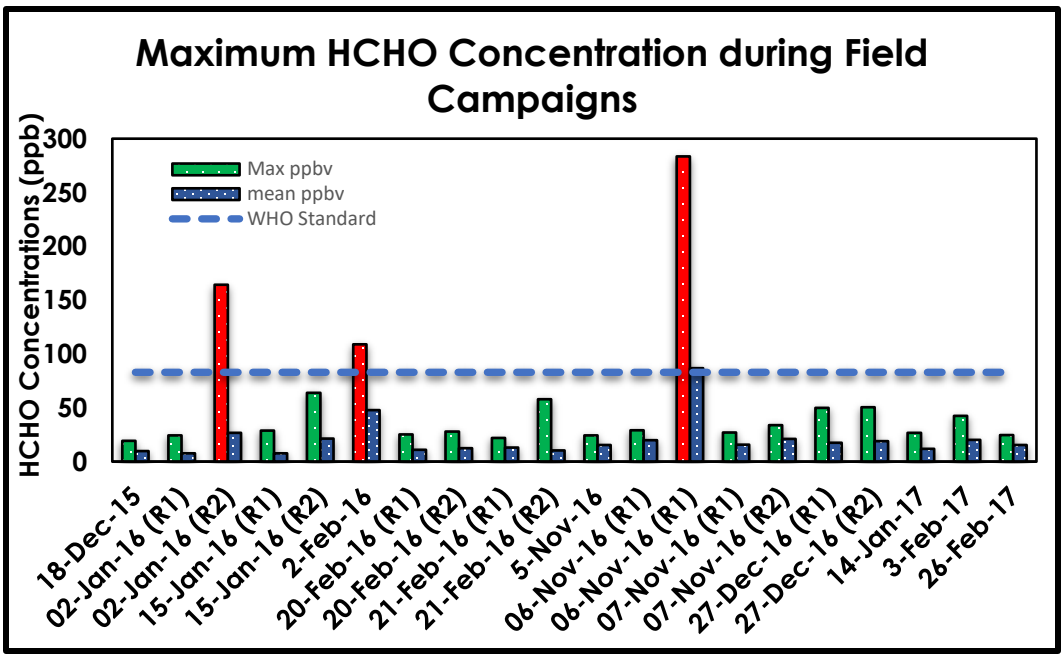

Figure 4.2: Maximum and mean HCHO concentration during field campaigns of Lahore city

Figure 4.2 shows the maximum and average values of concentration of CH_2O during all field campaigns conducted in Lahore city. The maximum concentrations of HCHO were found in the first round of 2nd February (108.99ppbv) and in the second round of 2nd January (164.33ppbv) and 6th November (283.53ppbv). The average values were also higher than WHO guideline on respective days. The possible reasons for these high values are congested traffic, industries, brick kiln and smog episode etc. Besides the above-mentioned campaigns, the remaining field campaigns exhibit the concentration of HCHO that is within the WHO permissible limits (83ppbv).

4.1.2. Field campaigns around the cities of Multan and Islamabad

The maximum value during the Multan city field visit was measured on 29th December 2017 near Muzaffargarh bypass which was 1.54 x 10^{17} (131.12 ppb) violating the WHO

permissible limit. While other four campaigns of Multan city depict HCHO concentrations much lower than the permissible limits as shown in figure 4.1.

On 2nd March 2017, the maximum HCHO value around Islamabad and Rawalpindi was observed to be 3.09 x 10^{16} (26.31 ppb) near Kacheri chowk Rawalpindi where another peak value was measured along Karal chowk express highway. The possible sources are traffic load on these loads.

Table 4.2: Maximum and average concentrations of HCHO over Multan & Islamabad observed during field campaigns

Location	Date	Distance (km)	Avg._NO_2 VCD (molec/cm^2)	Max_NO_2 VCD (molec/cm^2)	Max_NO_2 VCD (ppbv)
Multan (R1)	28-December 2016	51.56	1.10E+16	2.48E+16	21.12
Multan R2	29-December 2016	55	3.60E+16	1.54E+17	**131.12**
Multan	15-January 2017	49.97	1.49E+16	3.42E+16	29.12
Multan	04-February 2017	47.11	3.04E+16	7.14E+16	60.79
Multan	27-February 2017	50.92	1.77E+16	2.77E+16	23.59
Islamabad	02-Mar 2017	44.66	1.24e16	3.09E+16	26.31

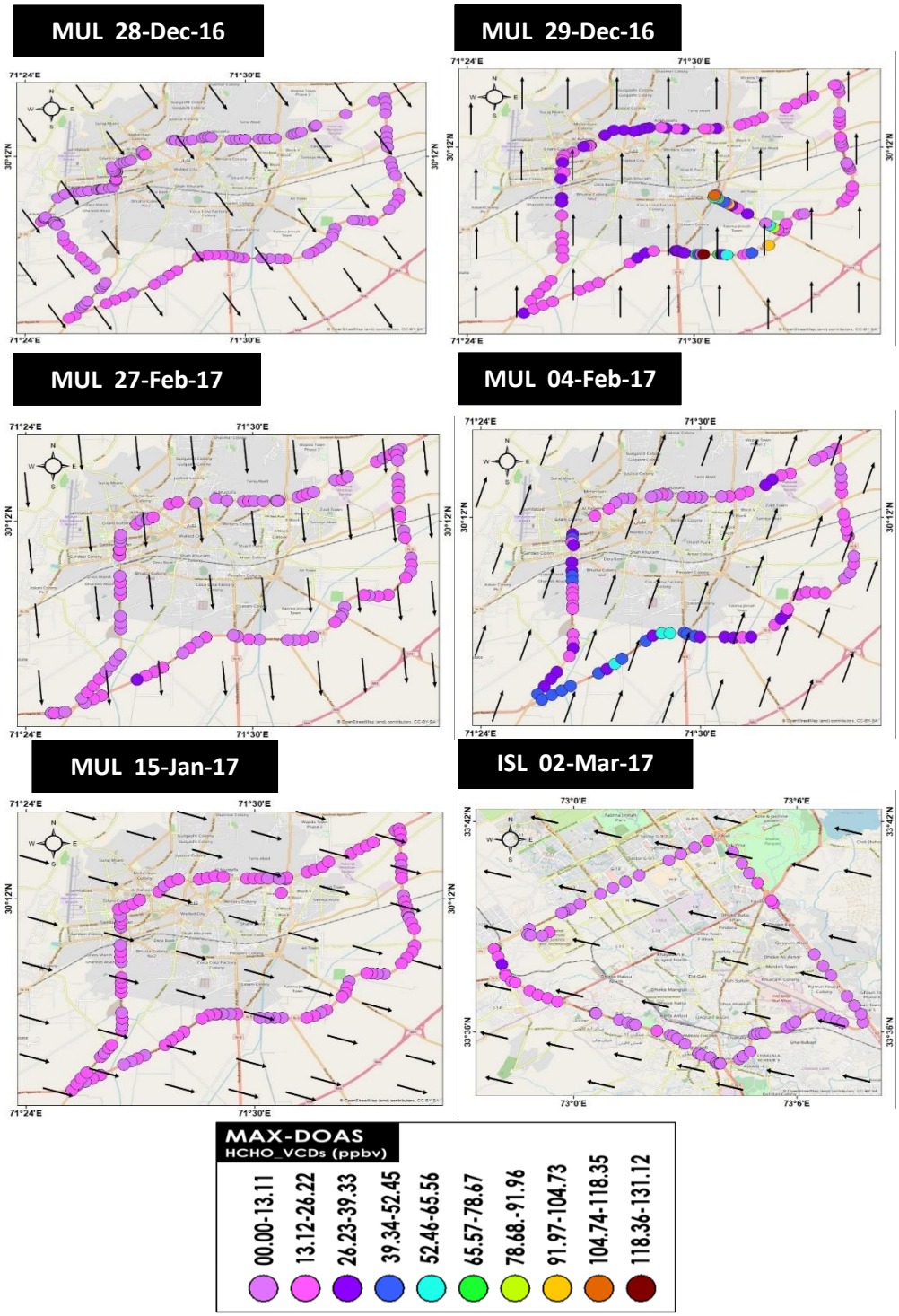

Fig 4.3: HCHO concentrations retrieved from car MAX-DOAS and OMI satellite observations conducted in the cities of Multan and Islamabad. Wind vectors are also included to represent the average wind direction during that field campaign observations.

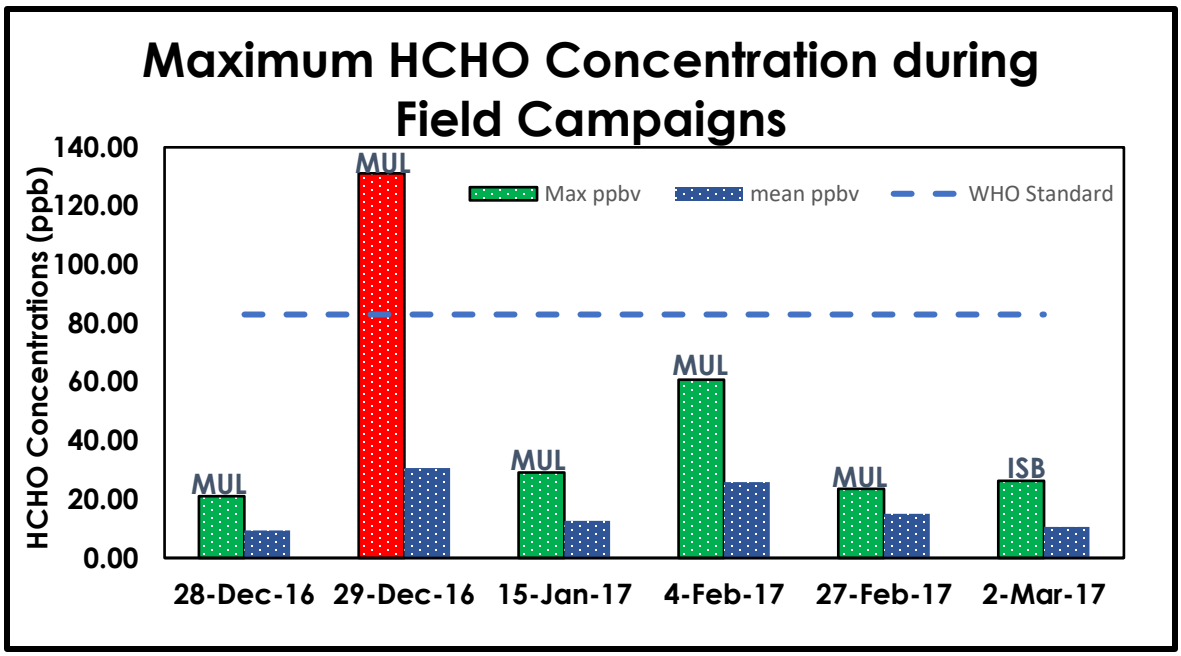

Fig 4.4: Maximum and mean HCHO concentration during field campaigns of Multan and Islamabad

Figure 4.4 indicates that only one field campaign in Multan city gave a much higher value of HCHO that is exceeding the threshold level defined by the WHO. The blue bar shows the average values of field campaigns. The plausible reason for this high value was emissions from a thermal power plant in Fatima fertilizer factory that use CNG as a fuel for power generation. To conclude, it was observed that during twenty periodic Lahore field visits from December 2015 to March 2017, the concentration of formaldehyde was observed much higher than the WHO limit, while out of six visits in Multan and Islamabad's field survey only one field campaign of Multan city shows a peak value above the WHO limits. So, in other words, the HCHO VCD values are significantly higher in Lahore followed by Multan and Islamabad.

4.2. **Diurnal Cycle of HCHO**

4.2.1. **Diurnal cycle of HCHO over Islamabad city**

The VCDs of HCHO are calculated from MAX-DOAS retrieved data for a period from September 2015 to August 2017 at IESE, NUST site. The hourly average of each day was taken to calculate the diurnal cycle of HCHO as shown in figure 4.5 (a). This graph depicts the annual diurnal cycle of Formaldehyde from 6 a.m. to 6 p.m. The concentration of HCHO was found to be at its maximum during early morning and evening. During early morning hours, apart from background concentrations of HCHO, it has not been removed at night because of absence of photolysis. At the initial hour formaldehyde concentration is declining and reached its minimum between 9-10 am because photolysis is dominant over oxidation of methane. As the temperature reaches to its optimal level during noon, biogenic emissions and OH radicals increase and they oxidize methane and produce formaldehyde as a by-product. The same justification was reported by Postylyakov et al., (2014).

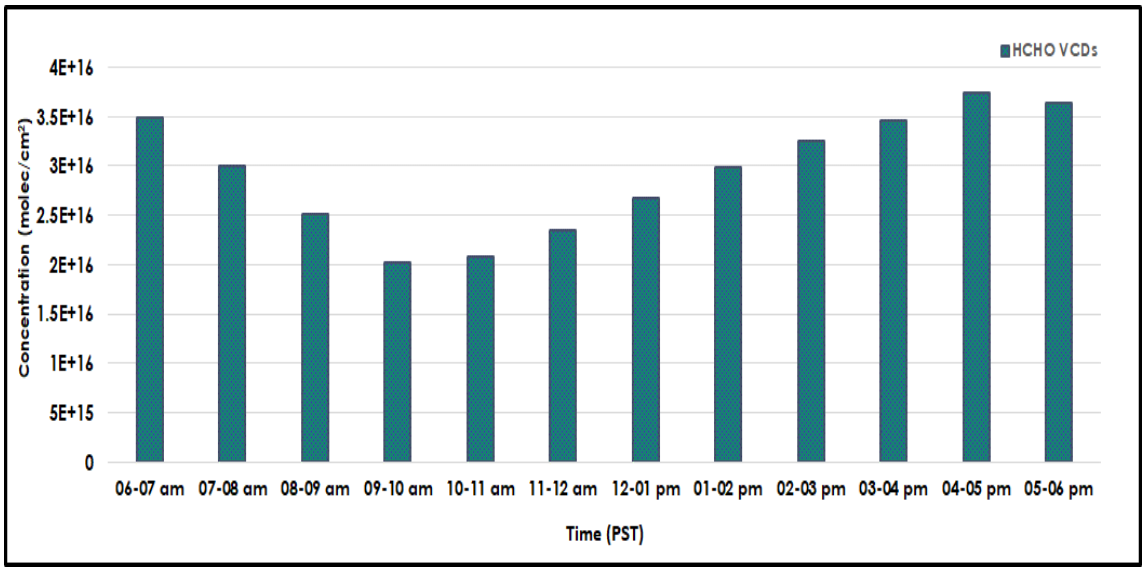

Fig 4.5(a): Avg. (6am to 6pm) diurnal cycle observed over IESE by MAX-DOAS

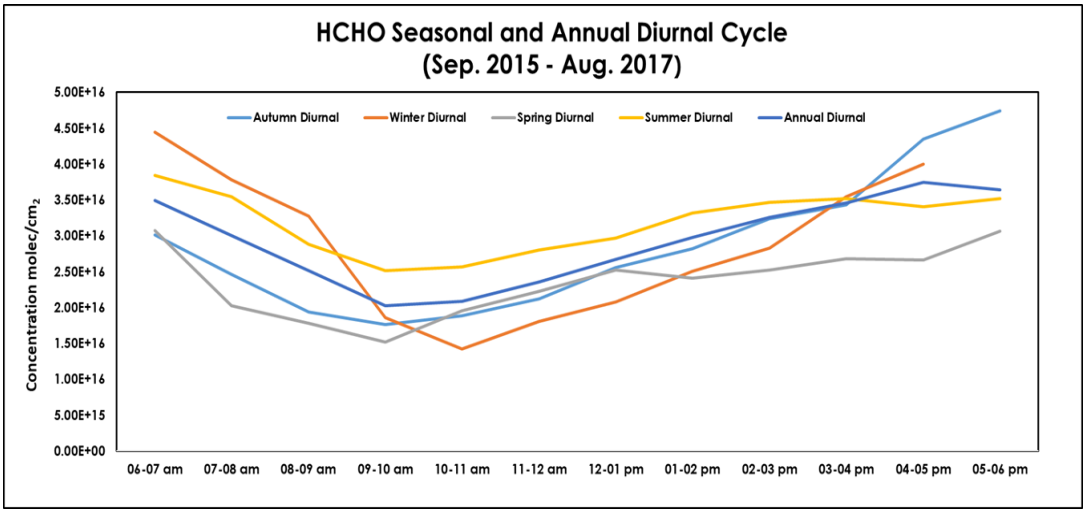

Fig 4.5(b): HCHO Seasonal and Diurnal Cycle (Sep. 2015 – Aug 2017) Over Islamabad

Fig 4.5 (b) shows that the seasonal diurnal cycle of HCHO also exhibits the maxima in summer season and minima in winter season due to temperature-driven biogenic emissions of isoprene and terpene. This also depicts that HCHO value is higher during early and late hours of winter months, this may be due to excessive use of natural gas in homes and offices for heating purposes because HCHO produces as a byproduct during oxidation of methane.

4.3. Weekly Cycle of HCHO

Average weekly cycle exhibited the maxima in weekdays and minima during weekends as shown in figure 4.6. The maximum values that observed during working are mainly due to the movement of people to offices, educational institutions, and personal businesses. While the minimum values that found during the weekend are due to public holidays in the capital city. In other words, the weekly cycle is significantly impacted by the transportation activities.

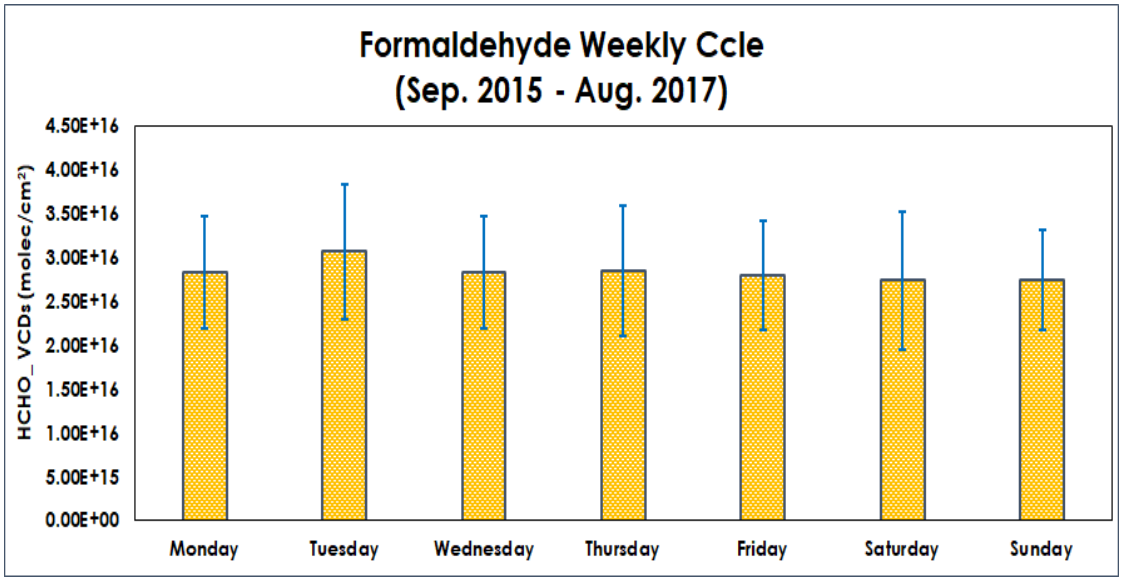

Figure 4.6: Weekly trend of HCHO concentrations over Islamabad monitored by MAX-DOAS

4.4. Monthly Temporal Cycle of HCHO

The monthly average temporal cycle from September 2015 to August 2017 exhibits that HCHO VCD values are higher in summer months followed by spring, fall and the winter are the lowest. (Leuchner *et al.*, 2016). The possible cause for high values in summer is driven by photochemistry that depends upon solar intensity, producing a large amount of secondary HCHO from methane and other present precursors. Besides these, some other precursor emitted from biogenic sources like isoprene is also in ample quantity in summer season (Luecken *et al.*, 2012).

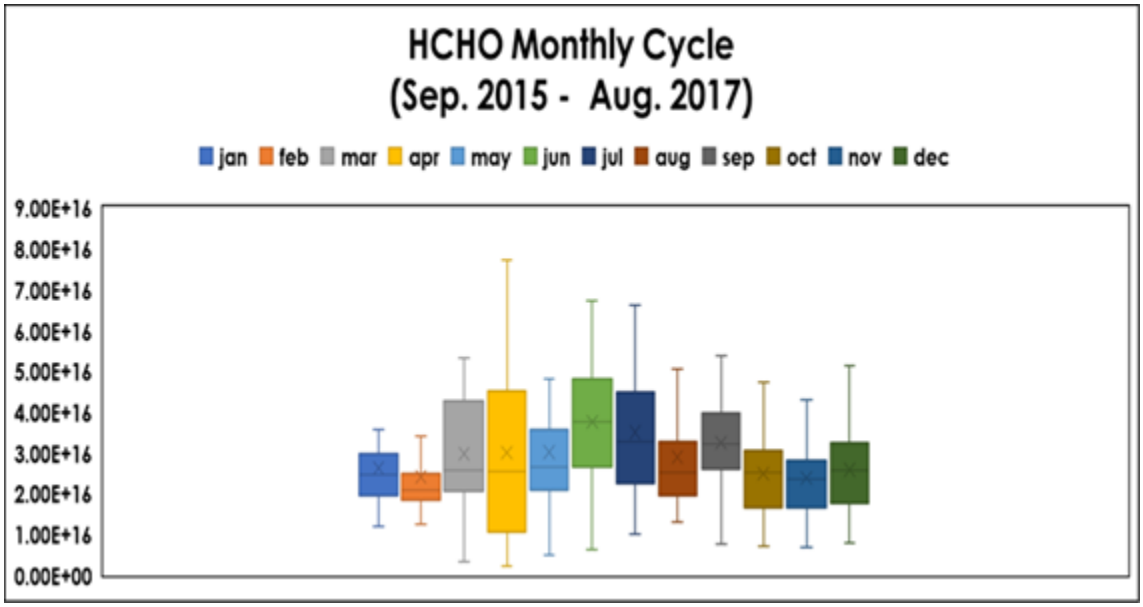

Figure 4.7: Formaldehyde Monthly averaged concentration over Islamabad (Sep. 2015 – Aug 2017) observed by Max-DOAS

4.5. Monthly Formaldehyde concentration and Wind rose over IESE, NUST

Figure 4.8a shows that in NE and NW direction from our sampling site is vegetation covered area, while ES and EW direction is congested population urban areas. In figure 4.8b, bar graph shows the monthly concentration of HCHO measured by Max-DOAS. While the Pie charts show the monthly wind rose measured by automatic weather station installed on roof top of USPCASE, NUST. It was observed that mostly maximum HCHO concentration was measured during that months in which wind was blowing from NE and NW directions. However, slightly less concentration was observed during that months in which wind blow from ES and SW. Wind speed also plays an important role in transportation of pollutant from one place to another. In some months, when wind blows

from urban area exhibited higher concentration because wind speed in higher as compared to other months.

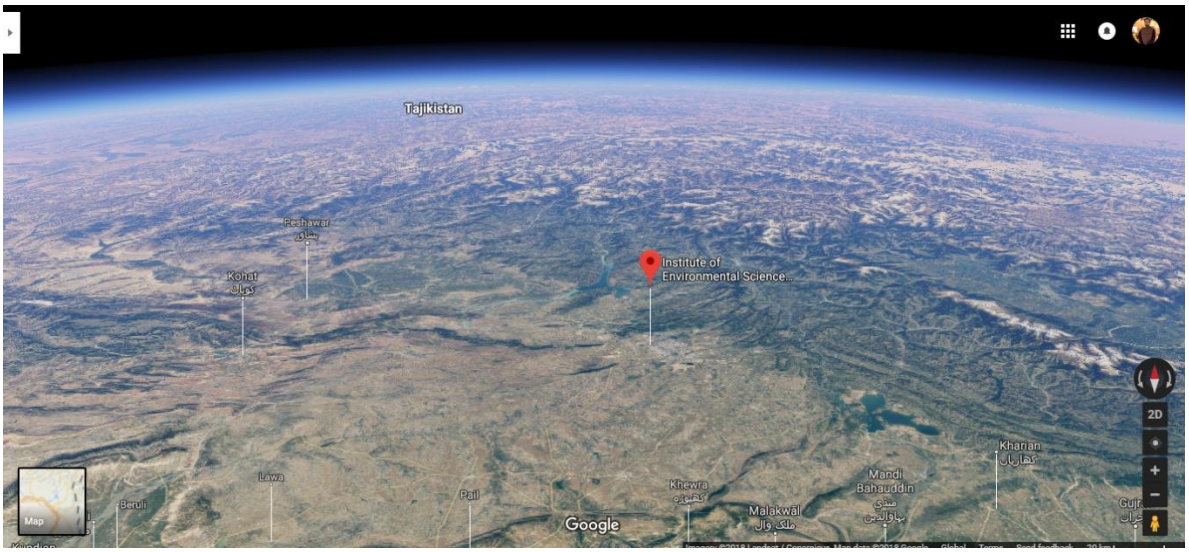

Figure 4.8a: 3D Google Map of Sampling site and its surrounding areas

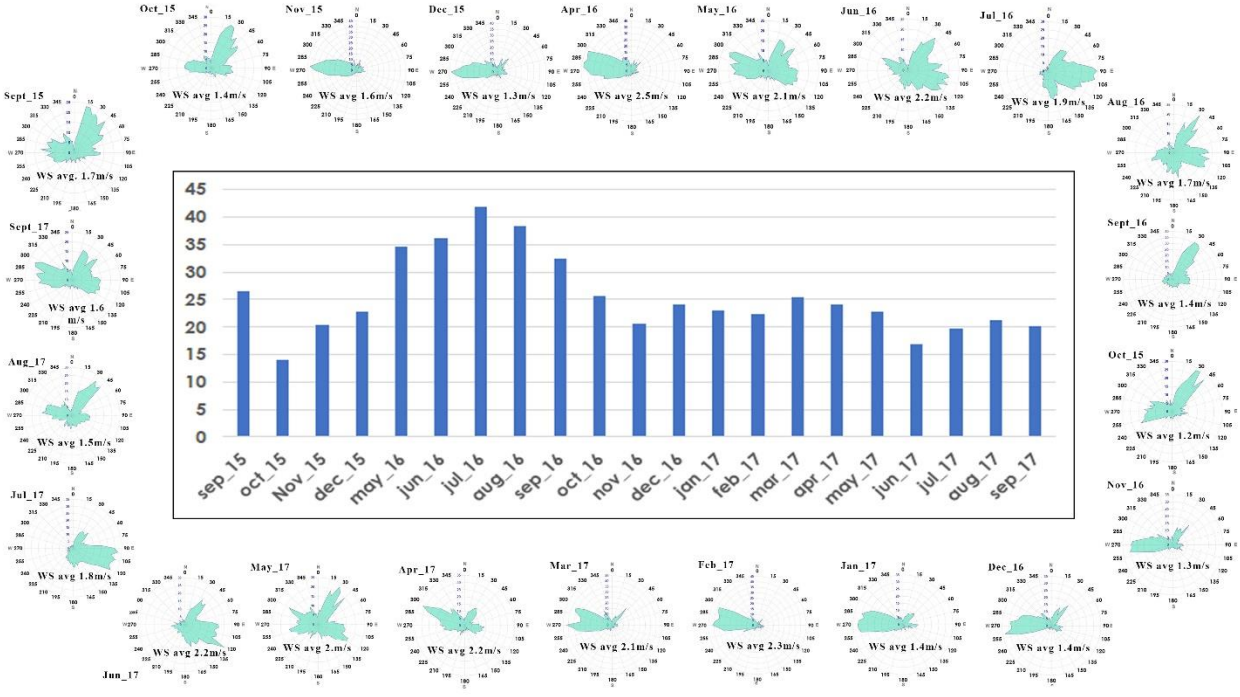

Figure 4.8b: Monthly Formaldehyde concentration and Wind rose over IESE, NUST over Islamabad

4.6. Satellite Validation of MAX-DOAS Data

4.5.1. HCHO Monthly Mean over Islamabad

OMI Satellite (0.25^{o}x 0.25^{o}) data obtained from TEMIS website as the average of each month above Islamabad. OMI satellite values for HCHO were underestimated as they were much lower than the MAX-DOAS values, may be due to aerosol shielding effect, clouds cover and the less sensitivity of satellite observations towards surface layers, However the trends of both OMI and MAX-DOAS concentrations were much more the same.

The monthly average of HCHO concentrations of MAX-DOAS and OMI satellite were compared. The satellite data for HCHO is available only from Sep. 2015 to Dec. 2016, hence OMI satellite data from only this time period was compared with MAX-DOAS, an average of 6am - 6pm time span. The person value "r" for this time span was 0.68 as shown in figure 4.8.

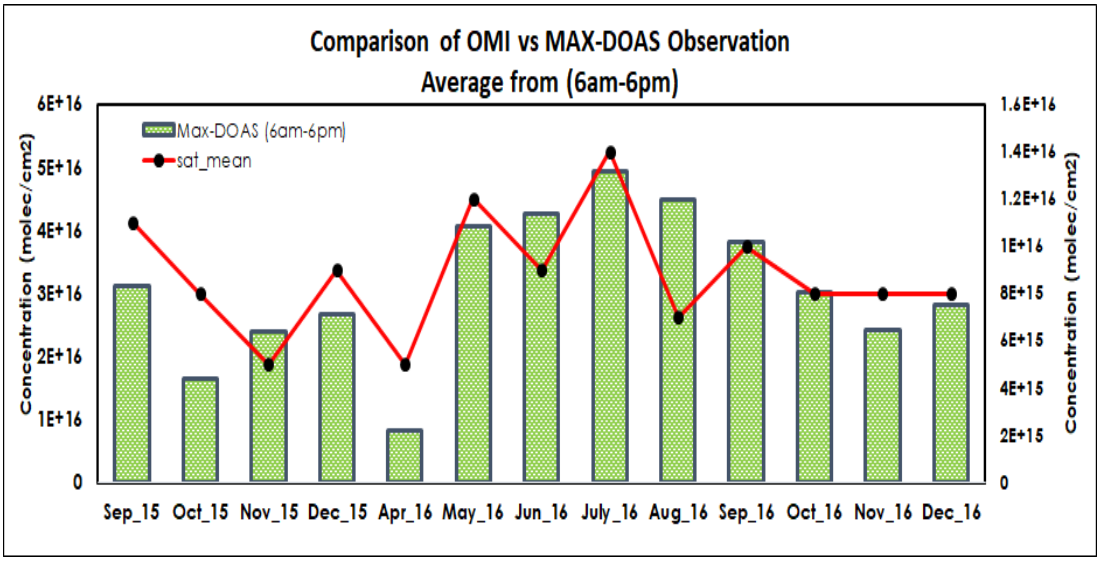

Figure 4.9a: HCHO monthly average of MAX-DOAS (6am to 6pm) vs OMI observations over Islamabad

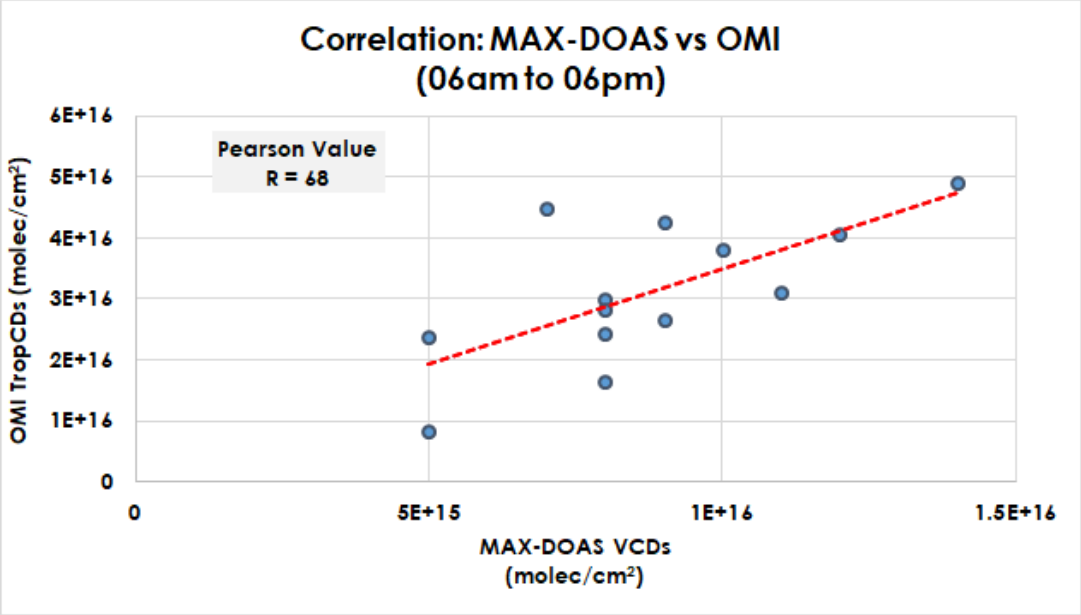

Figure 4.9b: Correlation of HCHO monthly average of MAX-DOAS (6am to 6pm) vs OMI over Islamabad

4.7. Plausible Sources of Formaldehyde

4.7.1. Intermediate Product in Methane Cycle:

Formaldehyde in the atmosphere is produced as a by-product during the methane cycle. In the atmosphere, methane is oxidized by hydroxyl radical producing methyl radical and water. Methyl radical, undergo different oxidation and reduction reactions in which methyl peroxide (CH_3O_2), methyl hydroperoxy (CH_3OOH), methyl oxide (CH_3O) are formed, finally produces formaldehyde (Seinfeld and Panels, 2008). Figure 4.10a confirm this thing that oxidation of methane triggers the amount of formaldehyde in the atmosphere. We compared the monthly MAX-DOAS concentration with industrial use of compressed natural gas (CNG) data and found a significant correlation of 0.70 as shown in figure 4.10b.

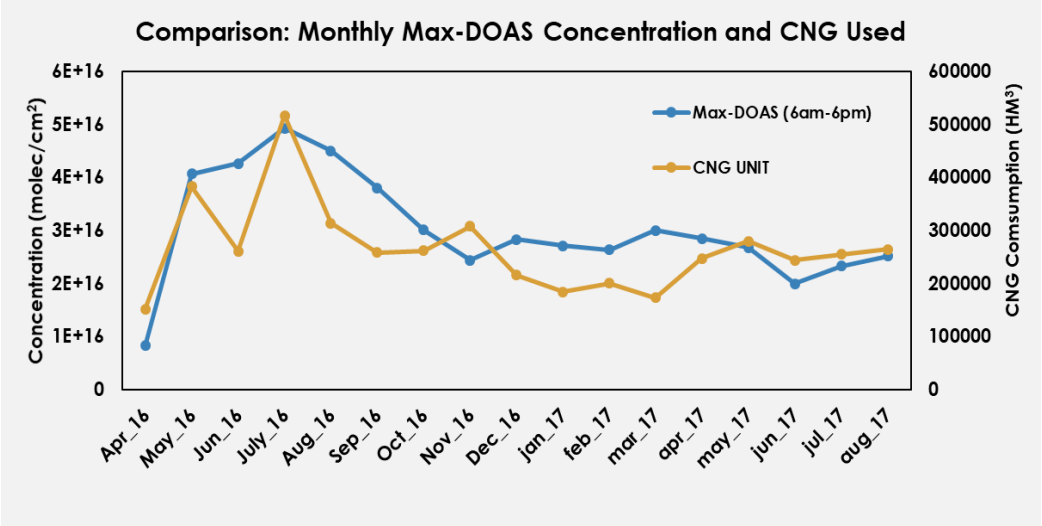

Figure 4.10a: Comparison of Monthly Max-DOAS concentration and Industrial CNG Consumed in Islamabad

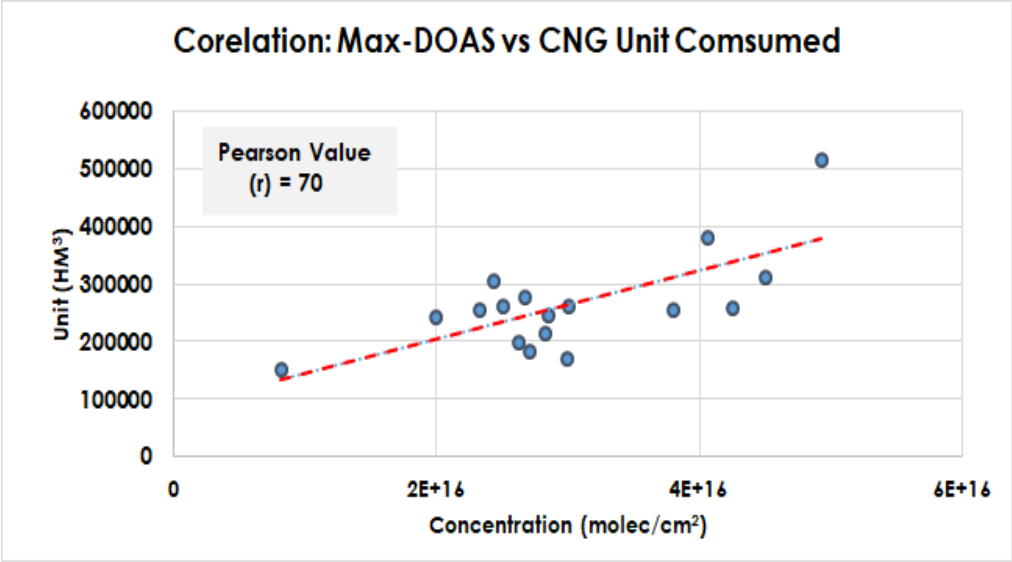

Figure 4.10b: Correlation of Monthly Max-DOAS concentration and Industrial CNG Consumed in Islamabad

4.7.2. Biogenic emissions from vegetation:

Biogenic emissions from vegetation are another source of formaldehyde. Figure 4.11a shows that NDVI and MAX-DOAS concentration depicts the similar variation. However, during high temperature and increased solar radiation, satellite tends to underestimate NDVI values because of heat stress on the plant and diminished chlorophyll contents. The

correlation of formaldehyde values from Max-DOAS showed a correlation of 0.68 with NDVI (Figure 4.11b).

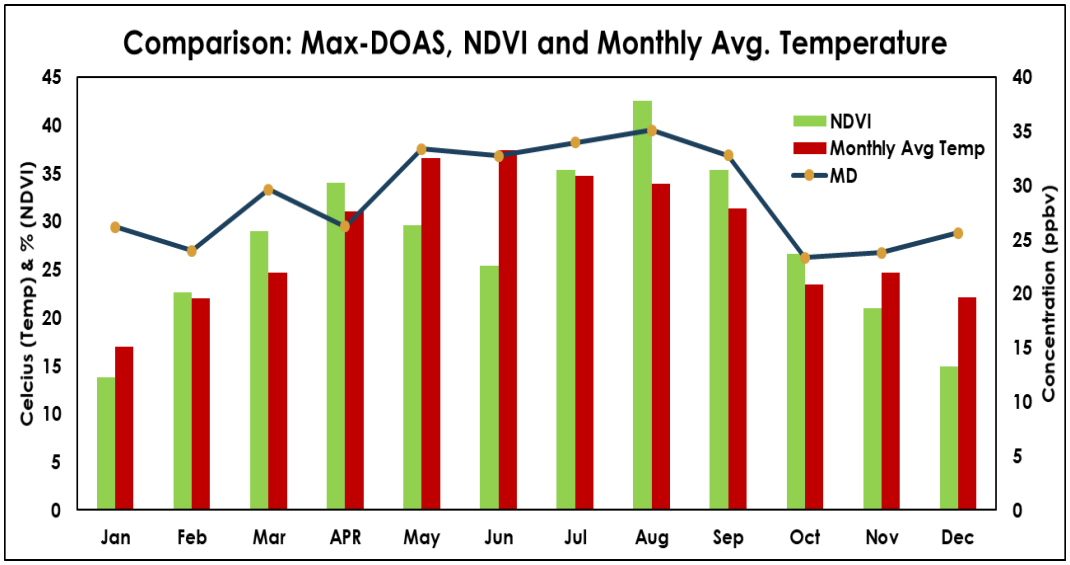

Fig 4.11a: Comparison of monthly Max-DOAS concentration, NDVI and monthly average temperature over Islamabad

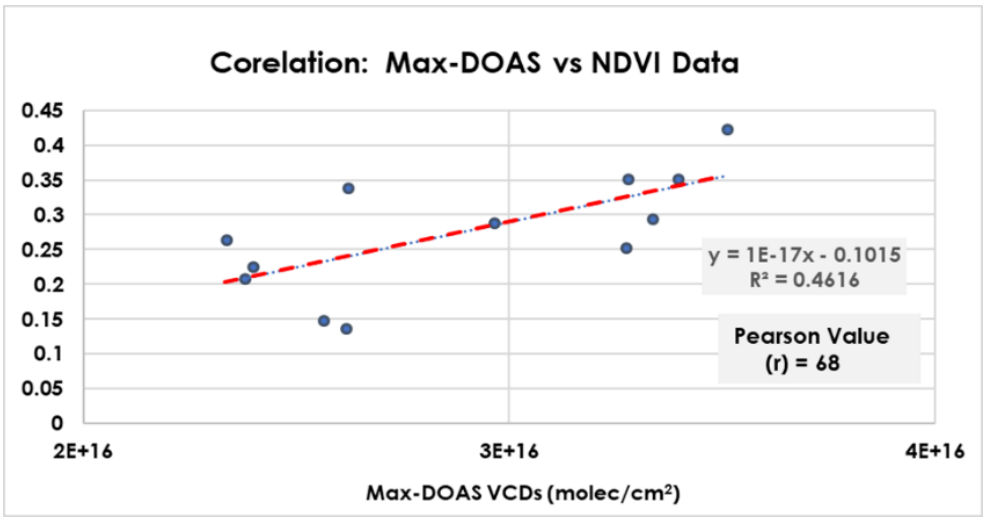

Fig 4.11b: Correlation of monthly Max-DOAS concentration, NDVI over Islamabad

Chapter 5

5. Conclusions and Recommendations

5.1. Conclusions

The car MAX-DOAS observation in Lahore, Multan and Islamabad along with a fixed monitoring point at IESE, NUST Islamabad were conducted to prepare a temporal record of HCHO concentration in the study area for the period of August 2015 to September 2017. In this work, formaldehyde vertical column densities attributed to potential sources in respective cities.

During Field campaigns in three megacities of Lahore Multan and Islamabad, HCHO concentration was observed maximum around the busy roads and industrial area. The maximum HCHO VCDS measured during field campaigns in Lahore were on 2nd January (164ppb), 2nd February (108ppbv) and 6th November 2016 (283ppb). While during Multan's field campaign the highest value was observed on 29th December 2016 (131ppb) exceeding the WHO permissible limit of 83 ppb. The possible reasons for these high values include vehicular emission, airports, industrial units and smog episode in the winter season of year 2016. As per observations of field campaigns at the three major cities of Pakistan: HCHO was measured highest in and around the Lahore city followed by Multan and Islamabad.

As fixed point (continuous) monitoring was also carried out at IESE, NUST Islamabad, which shows that HCHO concentration is within permissible limit of WHO. However, some peaks in daily data of HCHO concentration is due to wind, which transport the

pollutant away from the emission sources located in neighboring industrial area of I-9 Islamabad and Rawalpindi.

When compared with OMI satellite a similar spatial pattern was observed. The minor discrepancies are solely due to the fact that OMI gives us average observations whereas MAX-DOAS gives the point observations over a grid box of 0.25^{o} x 0.25^{o}.

5.2. Recommendations

The recommendations based on the findings in this study are:

- The results of this study may be used to detect, a connection between air pollutants and their sources, therefore, effective Pollution Control Techniques (PCTs) can be proposed for the abatement of air pollution in Pakistan.
- Air Quality Monitoring should be conducted on consistent basis, leading to the generation of an authentic national data base. NEQS of formaldehyde do not exist.
- Besides, an effective media campaign can also improve the people's understanding and concern about air quality.
- Furthermore, at different levels of the administration such as federal, provincial and local government level, air quality management plans should be introduced along with the effective utilization of atmospheric models in order to assess the real time status of air quality.
- A better understanding of the emissions of HCHO precursor from vegetation is needed, such as the terpenes, sesquiterpenes, and other highly organic compounds emitted by vegetation.

- By analyze the pollution profile of mega cities, we can estimate the pollution levels of the major cities. Also, the data can be used as a baseline by other research organizations, environmental agencies and Non-Government.

6. References

- Andreae, M. O., & Merlet, P. (2001). Emission of trace gases and aerosols from biomass burning. Global Biogeochemical Cycles, 15(4), 955-966.
- Apel, E. C., Calvert, J. G., Riemer, D., Pos, W., Zika, R., Kleindienst, T. E., ... & Roberts, P. T. (1998). Measurements comparison of oxygenated volatile organic compounds at a rural site during the 1995 SOS Nashville Intensive. Journal of Geophysical Research: Atmospheres (1984–2012), 103(D17), 22295-22316
- Ayres, J. G., Forsberg, B., Annesi-Maesano, I., Dey, R., Ebi, K. L., Helms, P. J., … & Forastiere, F. (2009). Climate change and respiratory disease: European Respiratory Society position statement. European Respiratory Journal, 34(2), 295-302.
- Bais, A. F., McKenzie, R. L., Bernhard, G., Aucamp, P. J., Ilyas, M., Madronich, S., & Tourpali, K. (2015). Ozone depletion and climate change: impacts on UV radiation. Photochemical & Photobiological Sciences, 14(1), 19-52.
- Bernstein, L., Bosch, P., Canziani, O., Chen, Z., Christ, R., & Riahi, K. (2008). IPCC, 2007: climate change 2007: synthesis report.
- Berman, E. S., Fladeland, M., Liem, J., Kolyer, R., & Gupta, M. (2012). Greenhouse gas analyzer for measurements of carbon dioxide, methane, and water vapor aboard an unmanned aerial vehicle. Sensors and Actuators B: Chemical, 169, 128-135.

- Boersma, K. F., Eskes, H. J., Veefkind, J. P., Brinksma, E. J., Van Der A, R. J., Sneep, M., ... & Bucsela, E. J. (2007). Near-real time retrieval of tropospheric NO_2 from OMI. Atmospheric Chemistry and Physics, 7(8), 2103-2118.
- Brune, W. H., Tan, D., Faloona, I. F., Jaeglé, L., Jacob, D. J., Heikes, B. G., ... & Blake, D. R. (1999). OH and HO_2 chemistry in the North Atlantic free troposphere. Geophysical Research Letters, 26(20), 3077-3080.
- Chimonas, G., & Rossi, R. J. (1989). Relationship between the midlatitude tropopause potential temperature and the thermodynamics of surface air. Journal of the Atmospheric Sciences, 46(14), 2135-2142.
- Choi, W., Faloona, I. C., Bouvier-Brown, N. C., McKay, M., Goldstein, A. H., Mao, J., & Millet, D. B. (2010). Observations of elevated formaldehyde over a forest canopy suggest missing sources from rapid oxidation of arboreal hydrocarbons. Atmospheric Chemistry and Physics, 10(18), 8761-8781.
- Clémer, K., Fayt, C., Hendrick, F., Hermans, C., Pinardi, G., & Van Roozendael, M. (2009, October). The simultaneous retrieval of tropospheric aerosol extinction and NO2 vertical profiles from MAXDOAS measurements in Beijing. In Proceedings of the 8th International Symposium on Tropospheric Profiling (pp. 19-23).
- Dobson, G. M. B., & Harrison, D. N. (1926). Measurements of the amount of ozone in the Earth's atmosphere and its relation to other geophysical conditions, 110(756), 660-693.
- Finlayson-Pitts, B. J., & Pitts Jr, J. N. (2000). Chemistry of the upper and lower atmosphere: theory, experiments, and applications. Academic press.

- Fu, T. M., Jacob, D. J., Palmer, P. I., Chance, K., Wang, Y. X., Barletta, B., ... & Pilling, M. J. (2007). Space-based formaldehyde measurements as constraints on volatile organic compound emissions in east and south Asia and implications for ozone. Journal of Geophysical Research: Atmospheres (1984–2012), 112(D6).
- Galloway, M. M., DiGangi, J. P., Hottle, J. R., Huisman, A. J., Mielke, L. H., Alaghmand, M., ... & Keutsch, F. N. (2012). Observations and modeling of formaldehyde at the PROPHET mixed hardwood forest site in 2008.Atmospheric Environment, 49, 403-410.
- Giorgi, F., Jones, C., & Asrar, G. R. (2009). Addressing climate information needs at the regional level: the CORDEX framework. World Meteorological Organization (WMO) Bulletin, 58(3), 175.
- Gurjar, B. R., & Lelieveld, J. (2005). New directions: megacities and global change. Atmospheric Environment, 39, 391-393.
- HANSLMEIER, A. (2007). The Earth's Atmosphere and Climate. In THE SUN AND SPACE WEATHER (pp. 123-142). Springer, Dordrecht.
- IARC (1995). Monographs on the Evaluation of the Carcinogenic Risk of Chemicals to Humans.Wood Dust and Formaldehyde. V 62. International Association for Research on Cancer., Lyon, France.
- World Health Organization. (2004). IARC monographs on the evaluation of carcinogenic risks to humans. Volume 88: Formaldehyde, 2-butoxyethanol and 1-tert-butoxypropan-2-ol. World Health Organization.
- Kovats, S., & Akhtar, R. (2008). Climate, climate change and human health in Asian cities. Environment and Urbanization, 20(1), 165-175.

- Larsen, J. C., & Larsen, P. B. (1998). Chemical carcinogens. issue I ENVIRONMENTAL SCIENCE AND TECHNOLOGY., 10: 33-56
- Lee, Y. N., Zhou, X., Kleinman, L. I., Nunnermacker, L. J., Springston, S. R., Daum, P. H., ... & Fehsenfeld, F. C. (1998). Atmospheric chemistry and distribution of formaldehyde and several multioxygenated carbonyl compounds during the 1995 Nashville/Middle Tennessee Ozone Study. Journal of Geophysical Research: Atmospheres (1984–2012), 103(D17), 22449-22462.
- Leuchner, M., Ghasemifard, H., Lüpke, M., Ries, L., Schunk, C., & Menzel, A. (2016). Seasonal and diurnal variation of formaldehyde and its meteorological drivers at the GAW site Zugspitze. Aerosol Air Quality Research, 16, 801-815.
- Li, X., Brauers, T., Hofzumahaus, A., Lu, K., Li, Y. P., Shao, M., ... & Wahner, A. (2012). MAX-DOAS measurements of NO2, HCHO and CHOCHO at a rural site in Southern China. Atmos. Chem. Physics Discussion, 12(2), 3983-4029.
- Luecken, D. J., Hutzell, W. T., Strum, M. L., & Pouliot, G. A. (2012). Regional sources of atmospheric formaldehyde and acetaldehyde, and implications for atmospheric modeling. Atmospheric Environment, 47, 477-490.
- Lu, Z., Streets, D. G., Winijkul, E., Yan, F., Chen, Y., Bond, T. C., ... & Carmichael, G. R. (2015). Light absorption properties and radiative effects of primary organic aerosol emissions. Environmental science & technology, 49(8), 4868-4877.
- Mellouki, A., Wallington, T. J., & Chen, J. (2015). Atmospheric chemistry of oxygenated volatile organic compounds: impacts on air quality and climate. Chemical reviews, 115(10), 3984-4014.

- Moran, M. D., Dastoor, A., & Morneau, G. (2014). Long-Range Transport of Air Pollutants and Regional and Global Air Quality Modelling. In Air Quality Management (pp. 69-98). Springer, Dordrecht.
- Olivier, J., Peters, J., Granier, C., Petron, G., Müller, J. F., & Wallens, S. (2003). Present and future surface emissions of atmospheric compounds. POET Rep. 2, EU Proj. EVK2-1999, 11.
- Piatt, U, & Stutz, J. (2008). Differential Optical Absorption Spectroscopy, Principles and Applications: Springer, Heidelberg.
- Postylyakov, O., & Borovski, A. (2014, November). Measurements of formaldehyde total content using DOAS technique: a new retrieval method for overcast. In Remote Sensing of the Atmosphere, Clouds, and Precipitation V (Vol. 9259, p. 925918). International Society for Optics and Photonics.
- Rom, W. N., Pinkerton, K. E., Martin, W. J., & Forastiere, F. (2008). Global warming: a challenge to all American Thoracic Society members. American journal of respirator and critical care medicine, 177(10), 1053-1054.
- Seinfeld, J. H., & Pandis, S. N. (2012). Atmospheric chemistry and physics: from air pollution to climate change. John Wiley & Sons. Sander, S. P., Friedl, R. R., Golden, D. M., Kurylo, M. J., Moortgat, G. K., Wine, P. H., ... & Keller-Rudek, H. (2006). Chemical kinetics and photochemical data for use in atmospheric studies evaluation number 15.
- Sheikh, I. M., Pasha, M. K., Williams, V. S., Raza, S. Q., & Khan, K. S. A. (2007). Environmental geology of the Islamabad-Rawalpindi area, northern Pakistan.

Regional Studies of the Potwar Plateau Area, Northern Pakistan, US Geological Survey, Reston, G1-G28.

- Solomon, S., Rosenlof, K. H., Portmann, R. W., Daniel, J. S., Davis, S. M., Sanford, T. J., & Plattner, G. K. (2010). Contributions of stratospheric water vapor to decadal changes in the rate of global warming. Science, 327(5970), 1219-1223.
- Stavrakou, T., Müller, J. F., Boersma, K. F., De Smedt, I., & van der A, R. J. (2008). Assessing the distribution and growth rates of NOx emission sources by inverting a 10-year record of NO_2 satellite columns. Geophysical Research Letters, 35(10)
- Stavrakou, T., Müller, J. F., De Smedt, I., Van Roozendael, M., van der Werf, G. R., Giglio, L., & Guenther, A. (2008). Evaluating the performance of pyrogenic and biogenic emission inventories against one decade of space-based formaldehyde columns. Atmospheric Chemistry & Physics Discussions,8, 16981-17036Brüne, B., von Knethen, A., & Sandau, K. B. (1999). Nitric oxide (NO): an effector of apoptosis. Cell Death and Differentiation, 6(10), 969.
- Vlemmix, T., Piters, A. J. M., Berkhout, A. J. C., Gast, L. F. L., Wang, P., & Levelt, P. F. (2011). Ability of the MAX-DOAS method to derive profile information for NO_2: can the boundary layer and free troposphere be separated? Atmospheric Measurement Techniques, 4(12), 2659-2684.
- Vlemmix, T., Piters, A. J. M., Stammes, P., Wang, P., & Levelt, P. F. (2010). Retrieval of tropospheric NO 2 using the MAX-DOAS method combined with relative intensity measurements for aerosol correction. Atmospheric Measurement Techniques, 3(5), 1287-1305.

- Vrekoussis, M., Wittrock, F., Richter, A., & Burrows, J. P. (2010). GOME-2 observations of oxygenated VOCs: what can we learn from the ratio glyoxal to formaldehyde on a global scale? Atmospheric Chemistry and Physics, 10(21), 10145-10160.
- Wayne, R. P., 2000: Chemistry of Atmospheres, Oxford University Press Inc., New York.
- Weber t schopp, a. et al. (1977). Irritant effects of formaldehyde on humans. International Archives of Occupational and Environmental health.,39: 207–218.
- World Health Organization. (1989). Proposed Air Quality Guidelines for Europe. World Health Organization Regional Office for Europe, Copenhagen.